NLD MP

S(200) JBS (3)

- Hiemstra, T., J.C.M. De Wit, and W.H. Van Riemsdijk. 1989b. Multisite proton adsorption modeling at the solid/solution interface of (hydr)oxides: A new approach. J. Colloid Interface Sci. 133:117.
- Hiemstra, T., and W.H. Van Riemsdijk. 1991. Physical chemical interpretation of primary charging behavior of metal (hydr)oxides. Colloids Surfaces 59:7–25.[ISI]
- Hiemstra, T., and W.H. Van Riemsdijk. 1996. A surface structural approach to ion adsorption: the charge distribution (CD) model. J. Colloid Interface Sci. 179:488–508.[ISI]
- Hiemstra, T., and W.H. Van Riemsdijk. 1999. Surface structural ion adsorption modeling of competitive binding of oxyanions by metal (hydr)oxides. J. Colloid Interface Sci. 210:182–193.[ISI][Medline]
- Hiemstra, T., and W.H. Van Riemsdijk. 2000. Fluoride adsorption on goethite in relation to different types of surface sites. J. Colloid Interface Sci. 225:94–104.[ISI][Medline]
- Hiemstra T., W.H. Van Riemsdijk, and G.H. Bolt. 1989a. Multisite proton adsorption modeling at the solid/solution interface of (hydr)oxides: a new approach. I. Model description and evaluation of intrinsic reaction constants. J. Colloid Interface Sci. 133:91–104.[ISI]
- Hiemstra, T., P. Venema, and W.H. Van Riemsdijk. 1996. Intrinsic proton affinity of reactive surface groups of metal (hydr)oxides: The bond valence principle. J. Colloid Interface Sci. 184:680–692.[ISI][Medline]

- Rietra, R.P.J.J., T. Hiemstra, and W.H. Van Riemsdijk. 1999b. Sulfate adsorption on goethite. J. Colloid Interface Sci. 218:511–521.[ISI][Medline]
- Rietra, R.P.J.J., T. Hiemstra, and W.H. Van Riemsdijk. 1999a. The relationship between molecular structure and ion adsorption on variable charge minerals. Geochim. Cosmochim. Acta 63:3009–3015.[ISI]
- Rietra, R.P.J.J., T. Hiemstra, and W.H. Van Riemsdijk. 2000. Electrolyte anion affinity and its effect on oxyanion adsorption on goethite. J. Colloid Interface Sci. 229:199–206.[ISI][Medline]

U.S.G.S. DENVER Library dlpark@usgs.gov Date of Request 6/21/06 236 5098

DAVID PARKHURST Patron's Name | MS 413 Location (MS and Bldg. no.) | WRD, BRR Div./Branch | Ext. Office | Ext. Messages

need by 6/30/06

AUTHOR; YEAR, PERIODICAL TITLE, VOL., PAGES

Call no. TITLE (of Book or Periodical Article)

Publisher (of Book)

SOURCE OF REFERENCE: Please include: Author, Date, Title, and Page of Book OR Title, Volume, Date, and Page of Journal.

FOR PHOTOCOPY REQUESTS – SIGN FORM ON REVERSE SIDE

(Initials of Library employee taking request AK

U.S. GEOLOGICAL SURVEY LIBRARY
WESTERN REGION
345 MIDDLEFIELD ROAD, MS-955
MENLO PARK, CALIFORNIA 94025-3591
REFERENCE: (650) 329-5027
CIRCULATION: (650) 329-5026
FAX: (650) 329-5132
(650) 329-5097
email: men_lib@usgs.gov

Diana Hisey
dhisey@usgs.gov
650-329-5034

Enclosed please find the article which you have requested. If you have a question or concern with the article, please contact me.

Notice: This material may be protected by copyright law (Title 17 US code). This document was scanned for your use and convenience and should not be shared with others. You may print a copy for your files or use the electronic copy on a temporary basis. This document should not be stored indefinitely as an electronic file.

5/2005
h:scansheet.doc

ISSN 0021-9797

This Number Completes Volume 179
Volume 179, Number 2, May 10, 1996

S(200)
J85
v.179
no.2

50 Years
1946-1996

JOURNAL OF Colloid and Interface Science

EDITOR-IN-CHIEF

Darsh T. Wasan
Illinois Institute of Technology, Chicago

CO-EDITORS

Arthur T. Hubbard
University of Cincinnati, Ohio

Josip P. Kratohvil
Clarkson University, Potsdam, New York

ADVISORY BOARD

Z. Adamczyk
Krakow, Poland

D. Attwood
Manchester, United Kingdom

J. B. Benziger
Princeton, New Jersey

R. P. Borwankar
Glenview, Illinois

D. Y. C. Chan
Parkville, Vic., Australia

C. G. de Kruif
Ede, The Netherlands

E. Dickinson
Leeds, United Kingdom

J. C. Eriksson
Stockholm, Sweden

F. Galembeck
Campinas, Brazil

F. M. Goñi
Bilbao, Spain

V. Hlady
Salt Lake City, Utah

J. P. Hsu
Taiwan, Republic of China

E. W. Kaler
Newark, Delaware

D. Langevin
Paris, France

M. Malmsten
Stockholm, Sweden

C. A. Miller
Houston, Texas

T. Seimiya
Tokyo, Japan

D. O. Shah
Gainesville, Florida

P. M. A. Sherwood
Manhattan, Kansas

V. Starov
Moscow, Russia

R. Strey
Göttingen, Germany

K. I. Tanaka
Tokyo, Japan

P. A. Thiel
Ames, Iowa

W. H. van Riemsdijk
Wageningen, The Netherlands

S. M. Yang
Taejon, Korea

Victor K. La Mer, Edito
Albert C. Zettlemoyer, Co-E
Milton Kerker, Co-Editor 1965–19

U.S. GEOLOGICAL SURVEY
MENLO PARK
MAY 29 1996
LIBRARY

ACADEMIC PRESS
San Diego New York Boston London Sydney Tokyo Toronto

JOURNAL OF COLLOID AND INTERFACE SCIENCE 179, 488–508 (1996)
ARTICLE NO. 0242

A Surface Structural Approach to Ion Adsorption: The Charge Distribution (CD) Model

T. HIEMSTRA[1] AND W. H. VAN RIEMSDIJK

Department of Soil Science and Plant Nutrition, Wageningen Agricultural University, P. O. Box 8005, 6700 EC Wageningen, The Netherlands

Received July 26, 1995; accepted October 18, 1995

An ion adsorption model for metal hydroxides has been developed which deals with the observation that in the case of inner sphere complex formation only part of the surface complex is incorporated into the surface by a ligand exchange reaction while the other part is located in the Stern layer. The charge distribution (CD) concept of Pauling, used previously in the multi site complexation (MUSIC) model approach, is extended to account for adsorbed surface complexes. In the new model, surface complexes are not treated as *point* charges, but are considered as having a *spatial* distribution of charge in the interfacial region. The new CD model can describe within a *single* conceptual framework *all* important experimental adsorption phenomena, taking into account the chemical composition of the crystal surface. The CD model has been applied to one of the most difficult and challenging ion adsorption phenomena, i.e., PO_4 adsorption on goethite, and successfully describes simultaneously the basic charging behavior of goethite, the concentration, pH, and salt dependency of adsorption, the shifts in the zeta potentials and isoelectric point (IEP), and the OH/P exchange ratio. This is all achieved within the constraint that the experimental surface speciation found from *in situ* IR spectroscopy is also described satisfactorily. © 1996 Academic Press, Inc.

Key Words: adsorption; model; cation; anion; proton; phosphate; speciation; heterogeneity; goethite; oxides; coordination; surface structure; double layer; spectroscopy.

INTRODUCTION

Cation and anion adsorption at the solid/solution interface of metal (hydr)oxides plays an important role in several fields of chemistry, including colloid and interface chemistry, soil chemistry and geochemistry, aquatic chemistry, environmental chemistry, catalysis, and chemical engineering. A large number of models, describing adsorption, is available (1–8). These differ in the formulation of the surface reactions and/or in the description of the electrostatic double layer. Further progress in the unification and development of models is desirable.

Various adsorption phenomena can be studied experimentally. Adsorption has frequently been studied as function of pH, and is either presented as adsorption isotherms or as so-called "adsorption edges." Such primary data are often fitted to an adsorption model. Given a limited data set, many models can often describe such data reasonably well. However, the underlying physical chemical nature of these adsorption models can be very different and additional information may help to discriminate between the various options. For instance, measurement of the electrolyte dependency of ion adsorption or the simultaneous release or uptake of protons may be informative since the experimental proton balance can be related to the change in particle charge. This type of information can be extended with measurements of the shift in electromobility and the resulting shift of the isoelectric point (IEP) following ion adsorption. The study of competition and synergistic adsorption of ions may also yield valuable additional information. Unfortunately such extended data sets for one particular ion and for one surface are not available. This limits the possibility of discriminating between the various models. At present, model development can only be achieved by a critical combination of data sets from various authors covering a broad range of adsorption phenomena.

An important aid to the process of model development is the availability of detailed molecular information about the ion adsorption mechanism resulting from powerful new *in situ* spectroscopic techniques. It has been known for quite sometime that ions, such as phosphate, may be adsorbed by ligand exchange (9–12). However, only recently quantitative data have become available for the surface speciation. For example, *in situ* cylindrical internal reflection–Fourier transformed infrared spectroscopy (CIR-FTIR) has shown that the binuclear bidentate $Fe_2O_2PO_2$ surface complex is the dominant adsorbed phosphate species at neutral pH values, and that one of the solution oriented ligands of this complex may be protonated at low pH (13). These measurements have also shown that the ratio of prononated/nonprotonated PO_4 surface complexes is dependent on the phosphate concentration. This detailed quantitative information will be used in the present paper.

The ligand exchange process can be considered as an obstacle in model development (14). It has usually been

[1] To whom correspondence should be addressed.

0021-9797/96 $18.00
Copyright © 1996 by Academic Press, Inc.
All rights of reproduction in any form reserved.

treated in a rather simplistic way, in the sense that the adsorbing ions have been treated as point charges. In the case of oxyanion adsorption, for example, only part of the adsorbing molecule is incorporated into the surface. This changes an OH(H) surface ligand into an oxygen O. It is clear from the structure of the interface that only part of the adsorbed molecule is incorporated into the surface structure while the other part is present in the so-called Stern layer. Here we extend the charge distribution approach of our earlier MUSIC model (15, 16) by including adsorbed surface complexes.

Additional useful information for model development may also be available from the solid side of the interface. The adsorption of ions is dependent on the crystal surface structure (17–22), which is related to the surface chemical composition. Several types of groups may be present at the surfaces and these may differ in their coordination with the metal (*Me*) ions of the solid bulk mineral. This implies that model parameters related to the surface composition (type and number of surfaces groups) will be determined by the crystal planes present. Therefore, the relevant model parameters should not be *a priori* available as free fitting parameters, but should be constrained by the physical chemical reality.

Based on the above considerations, we present a new model which can incorporate surface structural information. It treats both cation and anion adsorption in the same way and is based on the Pauling concept of charge distribution of ions over the coordinating ligands (23). It will therefore be referred to as the CD model. Phosphate adsorption on goethite has been chosen for testing and validating the CD model because it has been widely studied (9, 11, 13, 19, 24–28), it shows a complex adsorption behavior, and important new spectroscopic data for the phosphate surface complex have recently become available (13).

INTERFACE: BETWEEN SOLID AND SOLUTION

Classically a description of ion adsorption is based on well known ideas of the solution side of the interface. The principle concept is based on the treatment of ions as point charges. For instance, the overall charge ($z = -3$) of an oxyanion such as PO_4^{-3}, made up from a P^{+5} ion and four surrounding O^{-2} ions, can be thought to be centered at one point. The classical Gouy–Chapman treatment of the diffuse double layer (3, 29) is a typical example of the use of this concept. On the solid side of the interface the concept of charge distribution introduced by Pauling in 1929 (23) is used. The MUSIC model (15) applies this concept to charged interfaces. Our new CD model combines both of these concepts. Inner sphere complex formation, responsible for most specific ion adsorption phenomena, will be described using this concept of charge distribution. Ion pair formation, being more solution-side oriented, will be described in terms of point charges.

PROTONATION AND SURFACE CHARGE

Hydroxide and oxide interfaces are characterized by oxygens bound together by metal (*Me*) ions present in the bulk of the solid. The oxygens at the interface of (hydr)oxides may in principle bind protons in two consecutive steps, forming OH and OH_2 ligands, respectively. This may be written as

$$O^{-2} + 2H^+ \leftrightarrows OH^{-1} + H^+ \leftrightarrows OH_2^0. \qquad [1]$$

Equation [1] shows that the surface may contain O^{-2}, OH^{-1}, and OH_2^0. In variable charge models, the overall charge at the surface (σ_0) is a basic property which can be established by counting the number of the various types of groups and their corresponding charges that are present at the interface. On the basis of Eq. [1], it is not possible to do this *a priori* because the surface oxygen is not only partially neutralized by protons, but is also partially neutralized by the *Me* ion(s) in the mineral structure. Therefore, the total charge of the surface group depends on the degree of neutralization coming from the *Me* ion(s) in the solid. The question that now arises is how much charge from the *Me* ion(s) in the solid should be attributed to the O^{-2}, OH^{-1}, and OH_2^0 present at the interface. The answer depends on how the charge of O^{-2} and OH^{-1} in the solid is neutralized, as discussed below.

CHARGE DISTRIBUTION

Ionic crystals can be visualized as structures in which the interior ions are surrounded by neighbors of opposite sign. In stable oxide structures, the principle of electroneutrality implies that the charge of a cation is compensated by the charge of the surrounding oxygens. Therefore, the neutralization of the positive charge can be considered as being distributed over all the oxygens that coordinate to the cation. In turn, the charge of an oxygen is compensated by several cations and is therefore only partially neutralized by a single cation. If the degree of neutralization of charge is expressed per bond, the neutralization of the anionic charge will be equal to the sum of the coordinated cationic charges reaching the anion. This concept was introduced by Pauling (23) and is known as one of the Pauling rules (30). The symmetric distribution of charge over the surrounding bonds leads to the definition of a formal bond valence (ν) as the charge (z) of a cation divided by its coordination number (CN):

$$\nu = \frac{z}{\mathrm{CN}}. \qquad [2]$$

Application of the CD concept leads to the definition of surface groups and their corresponding charge. For example, in the crystal structure of goethite, the Fe^{+3} ions ($z = +3$) are surrounded by 6 O(H) ligands (CN = 6). Applying Eq.

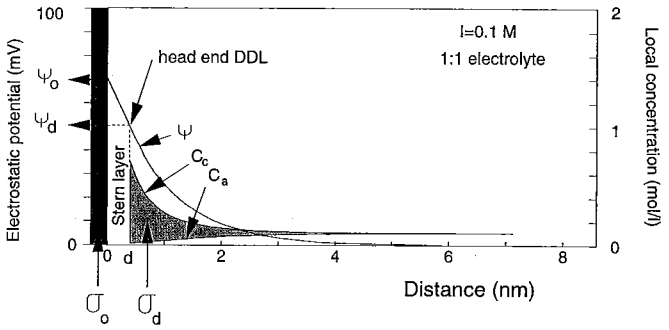

FIG. 1. An example of the calculated charge distribution at the surface as given by the basic Stern (BS) model. Surface charge (σ_0) is neutralized by charge in a double layer (σ_d). The double layer comprises an empty Stern layer which may be treated as a plate condenser and a diffuse double layer in which the counter- and co-ions are located. The Stern layer is limited by two electrostatic planes. H ions are adsorbed in the surface plane (called 0-plane). The electrostatic plane at the head end of the diffuse double layer is called the d-plane. The electrostatic potential (ψ) and electrolyte ion concentration (C_c and C_a) are given as function of distance from the surface. Although indicated as a rectangle with a given surface area, expressing an amount of charge, the surface charge σ_0 is theoretically located at a single position on the x-scale, i.e., located in a *plane* and not a *layer*.

[2], the charge per bond ν, attributed to one ligand will be $\nu = \frac{1}{2}$. At the surface of a mineral the oxygens can be coordinated to 1, 2, or even 3 Fe^{+3} ions in the bulk, leading to singly, doubly, and triply coordinated groups, respectively. Applying the charge attribution concept to the surface oxygens presented in Eq. [1] leads for singly coordinated oxygens to the following surface species:

$$Fe{-}O^{-3/2} + 2H^+ \leftrightarrows Fe{-}OH^{-1/2} + H^+ \leftrightarrows Fe{-}OH_2^{+1/2}. \quad [3]$$

The classical 2 pK models assume *a priori* an attribution of 1 unit charge per bond, leading to FeO^-, $FeOH^0$, and $FeOH_2^{+2}$ surface species.

DOUBLE LAYER STRUCTURE

As described above, surface oxygens are neutralized by both *Me* ions belonging to the solid and a variable number of adsorbed protons. Depending on the solution pH, an excess or a deficiency of protons may be present at the interface, which leads to a positively or negatively charged surface, respectively. This surface charge, σ_0 (Fig. 1), is compensated by electrolyte ions in a double layer, normally assumed to be a diffuse double layer (DDL). The formulations of the diffuse and the compact part of the double layer are given in the Appendix. The concentration of the counterions increases toward the surface (Fig. 1). The co-ion concentration follows the opposite trend. The ions present in the DDL are hydrated and have a finite size, thereby preventing charge neutralization starting directly from the close-packed *Me* (hydr)oxide surface. The counter- and co-ions ions have a distance of closest approach to the surface. This has led to the formulation of a charge free layer, called the Stern layer (31). This double layer picture has been described as the basic Stern (BS) model (32).

As indicated in Fig. 1, one may reach, even at low values of the surface potential, concentrations of 1 M or more at the head end of the DDL. From solution chemistry it is known that electrolyte ions at high concentration may form ion pairs. A similar situation is present at the interface where the electrolyte ions may pair with surface groups (33). This phenomenon of electrolyte ion/surface interaction has been confirmed by experiments (34, 35). The adsorbed ions are considered as outer sphere complexes, involving ligand–ligand interactions, so the adsorbed ion remains separated from the surface group by an O or H_2O ligand. This implies that these ion pairs have a similar minimum distance of approach as the counter- and co-ions of the DDL. From this point of view it is obvious that outer sphere complexes are adsorbed in an electrostatic plane positioned on the solution side of the Stern layer near the head end of the diffuse double layer. In the Gouy–Chapman concept of the DDL, ions are treated as point charges. We will also consider these charges as point charges.

Let us now focus on the position of the central ion of surface complexes formed by the interaction of cations and anions (for example Cd^{+2}, Al^{+3}, $H_4SiO_4^0$, SeO_3^{-2}, PO_4^{-3}, etc.) with the solid through ligand exchange (Fig. 2). These complexes are called inner sphere complexes (3). Due to ligand exchange, the inner sphere complexes are closer to the surface than the outer sphere complexes, leading to charge beyond the d-plane and within the Stern layer area. The inner sphere complexes are characterized by ligands which are shared between *Me* ions of the solid and the central ion of the adsorbed complex. These common ligands are in the same position as the other (protonated) surface oxygens, OH(H) of the *Me*OH and *Me*OH_2 surface species. The other, solution oriented, ligands of the adsorbed complex are located within the Stern layer region in a hypothetical electrostatic plane, called the 1-plane. The double layer picture would remain simple if the position of the 1-plane and the d-plane coincided. As will be shown later, the experimental data do not allow this simplification to be made if adsorption is to be described over a wide range of indifferent salt concentrations. The above double layer picture, consisting of three electrostatic planes (0-, 1-, and 2- or d-plane), will be called the three plane (TP) model.

THREE PLANE MODEL

In the three plane model, three electrostatic planes are present, enclosing two empty layers in terms of charge, each with its own electrostatic capacitance. In the absence of specifically adsorbing ions, the TP model simplifies to the

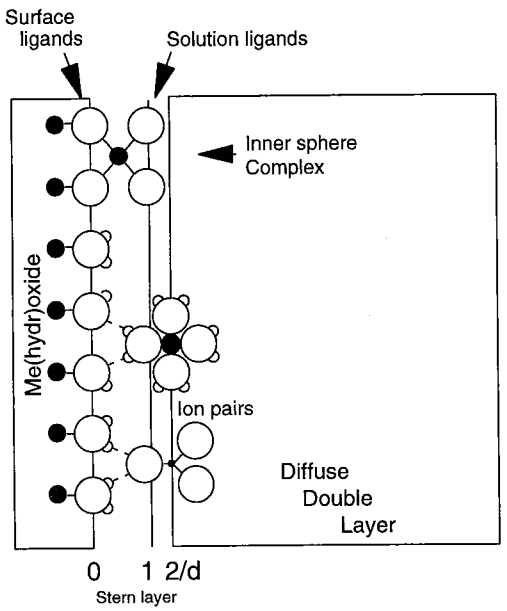

FIG. 2. A schematic representation of the location of outer sphere complexes and inner sphere complexes at the interface. The outer sphere complexes are present at a position determined by the minimum distance of approach of (hydrated) ions to a closely packed *Me* (hydr)oxide surface and are treated, like the ions in the DDL, as point charges in the CD model. The inner sphere complexes are closer to the surface, penetrating the Stern layer. The surface complexes formed by ligand exchange, have common ligand(s) present at the same electrostatic position as the surface oxygens. The other ligands of the surface complex are thought to be located in a plane within the Stern layer region, called the 1-plane.

BS model because the mid-plane does not contain any charge. The overall capacitance of the Stern layer region (C) in the BS and TP models, i.e., between the surface plane (0-plane) and the head end of the DDL (d-plane), can be found from classical acid–base titration data.

In the case of specific ion adsorption, the Stern layer region is divided into two layers separated by an electrostatic plane for the location of the solution-oriented ligands. The inner and outer layer capacitances, C_1 and C_2, respectively, are related to the overall Stern layer capacitance according to

$$\frac{1}{C} = \frac{1}{C_1} + \frac{1}{C_2}. \qquad [4]$$

The introduction of an additional electrostatic plane implies for the TP model that one of the capacitances of the two layers must be adjusted, while the other follows from Eq. [4], knowing the overall capacitance C from σ_0–pH data.

In the classical triple layer approach (33, 36–38), here referred to as the TL model, the capacitance of the outer layer (C_2) is set to 0.2 F/m^2. As has been pointed out by Hiemstra and VanRiemsdijk (39), this assumption is based on a misinterpretation of the relation between the double layer properties of AgI and that of *Me* (hydr)oxides. Analysis of the double layer properties of AgI and *Me* (hydr)oxides has shown that the very low value for the capacitance of AgI ($C \approx 0.2$ F/m^2) is due to the presence of strongly oriented water molecules in the first hydration shell of the Ag^+ and I^- ions of the solid. This strongly bound layer of hydration water is absent in the *Me*–hydroxide interface. It can be shown that for this reason, the overall capacitance of the Stern layer of *Me* (hydr)oxides is much greater than that of AgI. Our well crystalized goethite preparation gives an overall experimental capacitance of about 0.9 F/m^2 (BS approach).

LOCATING CHARGE

Once the location of complexes in the double layer has been defined, we can concentrate on the position of the charge. Part of the charge of an oxyanion complex, like adsorbed PO_4, is present in ligands shared with the surface. The charge of the remaining ligands is placed at the physical position of these ligands, i.e., the 1-plane. As explained above (Eqs. [1]–[3]), the charge on surface oxygens can generally be found by taking into account the charge of the oxygen ion, a proton (if present), and the contribution of the *Me* ion(s) on the solid side of the surface (Fig. 2). Extension of this concept to the Stern layer side of the surface implies that part of the neutralization of surface oxygens may be due to the presence of the central P^{+5} ion in the complex. A certain fraction f of the charge of the central cation in the complex will be attributed to the surface. The remaining part ($1 - f$) is attributed to the other ligands of the complex which are located in the 1-plane.

Several factors are responsible for the precise value of the charge distribution factor f of ions at the interface. A starting point is the Pauling bond valence concept (Eq. [2]). Let us apply this to an adsorbed silicic acid complex (Fig. 3).

In Pauling's bond valence concept, ions tend to distribute charge equally over the coordinating ligands. The value of the charge distribution factor f of the Si ion is then defined as $f = n\,\nu_{Si}$, in which n is the number of common ligands ($n = 1$ for a monodentate, $n = 2$ for a bidentate) and ν is the bond valence. In the case of an equal distribution (i.e., one charge unit per bond), half ($f = 0.5$) of the charge of the Si ion is attributed to two surface oxygens and the remaining half to the solution-oriented ligands. As indicated in Fig. 3 (case a) for an adsorbed bidentate silicon surface complex, this gives neutral solution-oriented ligands ($z_{OH} = 0$) and negatively charged surface-oriented ligands ($z_O = -0.5$). An equal distribution of charge may be in conflict with the Pauling concept of local neutralization of charge, which is related to the tendency of overall neutrality of the ligands in a solid. As a result of adsorption, the former surface ligands become "buried" and therefore will be more

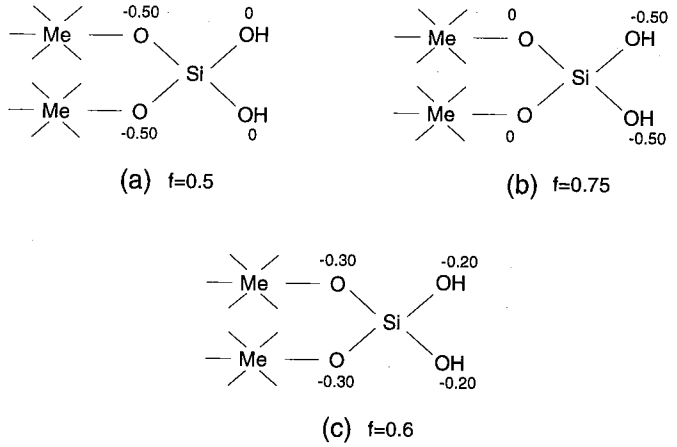

FIG. 3. A schematic representation of a bidentate silicon oxo complex bound to a *Me* hydroxide with trivalent *Me* ions in sixfold coordination ($\nu_{Me} = 3/6 = 0.5$). The charge of the various ligands is given for various choices of the value of the charge distribution factor f: (a) equal distribution of the charge of the central ion over the surrounding ligands; (b) an asymmetric distribution with neutral surface/solid oxygens; (c) the possible actual distribution with $f = 0.6$.

part of the solid. This implies that the surface ligands in the *Me*–ion surface complex may have a larger neutralization than the ligands on the solution side, leading to a larger value for f. If the common ligand in the solid/surface is fully neutralized, a situation as given in Fig. 3b would result, equivalent to $f = 0.75$. Actually for silicic acid adsorption on goethite the data imply a value for f of about 0.6. This value can be considered as a trade-off between the two opposing tendencies described above. The corresponding charge on the ligands for this asymmetric distribution of the charge on the central ion is shown in Fig. 3c. An additional complicating factor for a direct prediction of the value of f may be the presence of a covalent double bond in a surface configuration. Therefore f is treated as an adjustable parameter in the CD model.

So far we have not discussed the nature of the common ligands in a surface complex. If the common ligand is an oxygen, like the ones given in Fig. 3, we might call the complex an oxo complex. If the ligand is a common OH group, found for instance in a Cu^{+2} or Cd^{+2} surface complex, it will be called a hydroxo complex. The distinction between oxo and hydroxo complexes largely depends on the proton affinity of the common oxygen. The basic concepts of proton affinity are treated in our MUSIC model. The proton affinity is determined by the repulsive power(s) of the central ions surrounding the common O(H). Using the MUSIC model for estimating the log K values for protonation, it can be shown that the proton affinity of the common oxygen in an Fe–O–P or Fe–O–Si bond is too low to accept a proton in the normal pH range, while the proton affinity of an oxygen, bridging a Fe^{+3} and a divalent Cd ion, is high enough to give surface complexes with an OH as the common ligand, i.e., a Fe–OH–Cd linkage formed by the interaction of $FeOH^{-1/2}$ and Cd^{+2}. In the classical 2pK models, the formulated Me^{+2} surface complexes are quite different, since they are described as an Fe–O–*Me* linkage formed by FeO^- and Me^{+2} (37, 40).

A combination of the CD factor f with a knowledge of the type of ligands around the *Me* center (oxo versus hydroxo) can be used to calculate the changes in charge in the electrostatic planes during adsorption. This is required for the calculation of the electrostatic interaction energy of the adsorption reaction.

ADSORPTION ENERGETICS

The Gibbs free energy content, G, of a closed chemical system is composition dependent. At equilibrium the system is in its minimum Gibbs free energy state and the change of G with the extent of the reaction is zero, written as $\Delta G_r \equiv 0$. This change of G can be written in terms of a standard Gibbs free energy ΔG_r^0 and a composition dependent Gibbs free energy change ΔG_c. The latter term (ΔG_c) can be defined as $RT \ln Q$, in which Q is the reaction quotient, related to the entropy of mixing of species. For adsorption reactions of charged species the first term is influenced by changes in electrostatic energy, ΔG_{el} (1, 6, 42, 43). Formally, we may write for the equilibrium condition

$$\Delta G_r \equiv \Delta G_r + \Delta G_c \equiv \Delta G_r + RT \ln Q$$
$$\equiv \Delta G_r^0 + \Delta G_{el} + RT \ln Q = 0. \quad [5]$$

The standard Gibbs free energy change ΔG_r^0 can be connected by definition to the intrinsic reaction constant K_{in}, according to $\log K_{in} \equiv -\Delta G_r^0/2.3RT$. The electrostatic energy change, ΔG_{el}, is variable due to the change in charge upon adsorption of ions and is determined by the electrostatic potential ψ according to $zF\psi$. The potential is generally calculated with an electrostatic model, in which the charge distribution of ions is involved. In Eq. [5], the value of the reaction quotient Q is also variable, depending on the composition of the system. From a thermodynamic-statistical point of view the reaction quotient is generally expressed as

$$RT \ln Q = RT \ln \prod X_k^{r_k}, \quad [6]$$

where generally one chooses for X_k of a species k, its mole fraction M_k. For gases the mole fraction M_k is equivalent to the partial pressure P_k. For species in aqueous solution the molar concentration C_k is normally chosen as the parameter for X_k. In dilute aqueous systems C_k is directly proportional to the mole fraction M_k. The question is what should be chosen for X_k in the case of surface species.

REACTION QUOTIENTS OF MONO- AND BIDENTATE ADSORPTION REACTIONS

Spectroscopic information about the binding of ions to surfaces has indicated that adsorbed ions may share one (monodentate) or two (bidentate) common ligands with the solid. In the literature, the reaction quotient for the bidentate surface reaction is often not clearly formulated in terms of the exponent for the surface component and the suggested exponent ranges from 1 to 2 (28, 37, 41, 44). The definition of the reaction quotient, Q, should reflect (lattice) statistical effects as is done in the classical definitions of solution chemistry.

As an example we will write the formulations for phosphate adsorption which for the monodentate PO_4 adsorption can be written as

$$FeOH^{-1/2}(inf) + H^+(aq) + PO_4^{-3}(aq) \rightleftarrows FeO^pPO_3^q(inf) + H_2O(1) \quad K_1, \quad [7]$$

in which the index "inf" refers to the interface. The overall charge of the adsorption complex is attributed to the common oxygen in the surface (p) and three oxygens in the Stern layer (q). The sum of the charges p and q equals -2.5. The value of the overall reaction constant K_1 is a combination of the intrinsic constant K_{in1} and the (variable) electrostatic contribution, which depends on the location of the charge. One may write $K \equiv e^{-\Delta G_{ads}/RT} \equiv e^{-(\Delta G_r^0 + \Delta G_{el})/RT} \equiv K_{in}e^{-\Delta G_{el}/RT} \equiv K_{in}K_{el}$. The definition of the reaction quotient Q for Eq. [7], in combination with the chemical equilibrium condition $\Delta G_r = 0$ or $K = Q$, leads to

$$K_1 = Q = \frac{\theta_{FeO^pPO_3^q}}{\theta_{FeOH}} \frac{(H_2O)}{[H^+][PO_4^{-3}]}, \quad [8]$$

in which $[H^+]$ is the proton concentration, $[PO_4^{-3}]$ the concentration of PO_4^{-3} ions in solution, and (H_2O) the activity of water (a mole fraction). Because of the statistical origin of the entropy contributions, the concentration of surface species in Eq. [8] has been defined on the basis of a mole fraction. This mole fraction θ_i for surface species i reacting with a type of surface group j can be defined generally as

$$\theta_i = S_i/N_{s,j}, \quad [9]$$

in which S_i (mol/m^2) is the surface concentration of a species and $N_{s,j}$ the site density (mol/m^2) of surface group j.

In the case of monodentate adsorption, the definition based on mole fractions is equivalent to other definitions based on for instance mol/m^2, mol/g, or mol/liter, because the units by which the surface species are represented cancel. This is not true for bidentate reactions.

The binding of phosphate in a bidentate complex can be written as

$$2FeOH^{-1/2}(inf) + 2H^+(aq) + PO_4^{-3}(aq) \rightleftarrows Fe_2O_2^pPO_2^q(inf) + 2H_2O(1) \quad K_2, \quad [10]$$

in which two H^+ ions protonate the two surface OH groups forming chemically sorbed water which can be released in favor of two oxygens of PO_4. In this case the sum of p and q equals -2. The reaction quotient Q in combination with the equilibrium condition can be defined as in Eq. [8],

$$K_2 = Q = \frac{\theta_{Fe_2O_2^pPO_2^q}}{\theta_{FeOH}^2} \frac{(H_2O)^2}{[H^+]^2[PO_4^{-3}]}, \quad [11]$$

in which the square term for θ_{FeOH}, resulting from the mass law, expresses the probability of finding two surface groups together in the same configuration in the lattice.

The thermodynamic constant should be independent of the experimental conditions such as the solid/solution ratio (g/liter), surface area (m^2/liter), etc. This is true providing that mole fractions are used in the definition of K rather than mol/liter, mol/g, or mol/m^2. It is shown in the Appendix how this choice of unit may affect the calculations as formulated in the table of species.

Recent CIR-FTIR spectroscopic data have shown that one of the ligands of a phosphate bidentate complex may be protonated at low pH. The reaction defined in Eq. [10] can be extended by adding an extra proton which is needed to form the protonated ligand (OH):

$$2FeOH^{-1/2}(inf) + 2H^+(aq) + PO_4^{-3}(aq) + H^+(aq) \rightleftarrows Fe_2O_2^pPOOH^q(inf) + 2H_2O(1) \quad K_3. \quad [12]$$

This additional proton, written separately from the other protons in Eq. [12], will protonate one of the solution-oriented oxygens. It will give rise to a distinct electrostatic energy change (another Boltzmann accumulation factor) because it is not related to the 0-plane position, as both other protons are.

The corresponding reaction quotient and equilibrium condition for the above reaction is

$$K_3 = Q = \frac{\theta_{Fe_2O_2^pPOOH^q}}{\theta_{FeOH}^2} \frac{(H_2O)^2}{[H^+]^3[PO_4^{-3}]}. \quad [13]$$

The difference between the log K values for the protonated (log K_3) and nonprotonated bidentate phosphate complex (log K_2) is related to the proton affinity constant for the protonation of the solution-oriented ligand (log K_{Hp}). One may write log K_{Hp} = log K_3 − log K_2. This log K_{Hp} is related

to the experimentally determinable (CIR-FTIR spectroscopy) ratio of $Fe_2O_2PO_2$ and Fe_2O_2POOH.

In summary, the changes in Gibbs free energy are the sum of the contributions of the changes in standard Gibbs free energies ΔG^0_{ads} of adsorption (related to the intrinsic reaction constants K_{in}), changes in electrostatic energy ΔG_{el} (to be calculated), and changes related to the entropy of mixing $RT\ln Q$. The concentrations of the surface components are best defined in terms of mole fractions (θ).

In the CD model, calculation of the electrostatic energy ΔG_{el} differs from the classical approach and is discussed in the next paragraph.

ELECTROSTATICS

In the CD model, the electrostatic energy contribution (ΔG_{el}) is related to the electrostatic work done/released when the charge at position i with a certain potential (ψ_i) is changed by Δz_i according to

$$\Delta G_{el} = \Sigma \frac{\Delta z_i F}{RT} \psi_i . \qquad [14]$$

In terms of the electrostatic contribution to the K value of the reaction this contribution equals $K_{el} = e^{-\Delta G_{el}/RT} = e^{-\Sigma \Delta z_i F \psi_i / RT}$ in which $e^{-F\psi_i/RT}$ is the Boltzmann accumulation factor. In the cases where the adsorption contributes charge to different planes with different potentials, we have to know the individual charge attribution to each of these planes. This can be found by analyzing the change in charge resulting from surface complex formation. The net charge may change due to both adsorption and desorption reactions. The change of charge in the 0-plane (Δz_0) as a result of adsorption can be defined as

$$\Delta z_0 = \Delta n_H z_H + f z_{Me} \qquad [15]$$

and for the 1-plane (Δz_1) as

$$\Delta z_1 = (1 - f) z_{Me} + \Sigma m_j z_j, \qquad [16]$$

where Δn_H is the change in the number of protons on the surface ligand(s) involved in the surface reaction, z_H is the valence of the proton (+1), and f the charge distribution fraction. The change n_H depends on the number of common ligands (mono- or bidentate) and the change in the state of protonation of these ligands. The value of Δn_H may be positive, zero of negative. In Eq. [15] and Eq. [16], z_{Me} is the valence of the central ion in the surface complex. In Eq. [16], m_j is the number of ligands positioned in the 1-plane and z_j is the charge on those ligands (z_j = 0, −1, or −2, respectively, for an OH^0_2, OH^{-1}, or O^{-2} ligand).

As an example, we will derive the values of Δz_0 and Δz_1 for the bidentate phosphate adsorption reaction (Eq. [10]) in which two OH surface ligands are changed into two oxygens. This reaction implies a net release of two protons, i.e., $\Delta n_H = -2$. Knowing the value of the charge distribution fraction f of the central ion (f = 0.5 for P in $Fe_2O_2PO_2$), the change in charge z_0 in the surface or 0-plane can be found by applying Eq. [15]: $\Delta z_0 = [(-2)\cdot(+1)] + [(0.5)\cdot(+5)] = 0.5$. The corresponding Boltzmann accumulation factor therefore equals $e^{-0.5F\psi_0/RT}$. Similarly we may find the change in charge in the 1-plane (Δz_1). The charge is due to the ligands O^{-2} and/or OH^{-1} and their partial neutralization by the central ion $(1 - f)\, z_{Me}$. In the case of $Fe_2O_2PO_2$, Eq. [16] gives $\Delta z_1 = [(1 - 0.50)\cdot(+5)] + [(2)\cdot(-2)] = -1.5$ and a Boltzmann factor of $e^{+1.5F\psi_1/RT}$. The derived value of Δz_0 can also be found following the change of charge resulting from the different steps of the reaction: adsorption of protons resulting in the formation of two OH^0_2 ligands (+2), release of both neutral OH^0_2 ligands (−0), placement of two O^{-2} [(2)·(−2)] ligands, and partial neutralization by P [(0.5)·(+5)], yielding $\Delta z_0 = [+2] + [-0] + [(2)\cdot(-2)] + [(0.5)\cdot(+5)] = +0.5$.

The calculated values Δz_0 and Δz_1 can be used to find the actual charges p and q on the ligands of the surface complex (Eq. [10]). The sum of both initial charges (−0.5) on the common O ligands before reaction and the change of charge Δz_0 (=0.5) gives $p = [(2)\cdot(-0.5)] + [0.5] = -0.5$. The value of q equals Δz_1 resulting in $Fe_2O_2^{-0.5}PO_2^{-1.5}$.

Besides surface species, species in solution also play a role in adsorption. Generally ions in solution do not behave ideally due to mutual interactions, especially at higher ionic strengths (I). This interaction energy can be calculated by applying the Debye–Hückel theory for charged ionic species. It is introduced in the equilibrium condition by using activities, a_k, instead of concentrations, c_k, with $a_k = f_k c_k$ in which f_k is the activity coefficient of the ion species k. For $I > 0.1\ M$ an additional empirical correction has to be introduced as is done in the Davies equation (45).

Adsorption on variable charge surfaces can be calculated with the CD model using the ECOSAT chemical speciation program, based on a modified approach of Westall and Hohl (32). The fractional charges of surface components are incorporated with a *single minor* change (see Appendix).

SITES AND SURFACE STRUCTURE

The chemical reactivity of interfaces is determined by the type and number of surface groups present, which in turn is related to the type of crystal planes present. A number of experimental studies have determined the crystal morphology of goethite in some detail. Electron microscopy shows that goethite crystals are elongated in the c axis direction giving a needle-like shape. Early work on goethite (46) suggested that the 100, 010, and 001

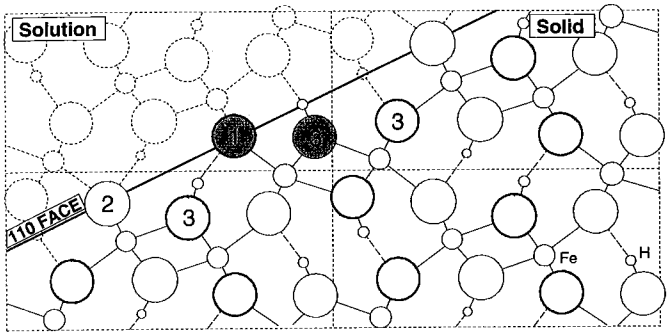

FIG. 4. A schematic representation of the cross section of goethite perpendicular to the *c* axis showing the surface structure of the 110 face. The ions that have been removed from the structure in order to illustrate the composition of the interface are shown by fine dashed lines. In the solid, the oxygens (large circles) are triply coordinated with Fe^{+3} (only two Fe–O bonds are shown). The bold circles indicate a raised position in the lattice. Half of the oxygens have a proton attached (OH). At the interface a lower coordination number (CN) is found. The CN is indicated by the numbers 1, 2, or 3 which identify the singly, doubly, or triply coordinated oxygens, respectively. The shaded surface oxygens are considered to be proton reactive (see text).

crystal faces were dominant. More recently, electron microscope (EM) studies of cross sections of goethite needles perpendicular to the elongated *c* direction have shown that the dominant crystal plane is the 110 plane which holds not only for synthetic but also for naturally formed crystals (47–54). EM studies of the goethite preparation used in this study confirmed the presence of predominantly 110 faces. At the end of the needles the 021 plane is found.

Knowing the dominant crystal face, one may assess the chemical composition of the surface by cutting an imaginary cross section of the crystal in the appropriate direction. The composition may be identical (Fig. 4) with the cut yielding the highest Fe density parallel to the 110 direction, as is done classically. On a unit cell basis, there are 3 rows of triply coordinated surface $Fe_3O(H)$ groups in the *c* direction, one row with singly coordinated FeOH(H) surface groups and one row with doubly coordinated surface Fe_2OH groups.

As indicated in Fig. 4, the 110 face will have one doubly coordinated Fe_2OH^0 surface group per unit cell length. It has been shown earlier (15), based on estimates of the proton binding constants of the doubly coordinated surface groups, that these doubly coordinated surface groups are essentially inert and zero charged; i.e., over a very wide pH range the dominant doubly coordinated surface species is Fe_2OH^0.

The goethite surface is dominated by triply coordinated surface $Fe_3O(H)$ groups (Fig. 4) and this will be reflected in the value of the PZC. The PZC of the goethites used in our study is high (9 ± 0.5) indicating a high value for the log *K* of the protonation reaction of triply coordinated surface groups. This contrasts with the low value for Fe_3O, predicted by the MUSIC model (15). It is reasonable to assume that the triply coordinated groups that have different positions in the surface structure may also differ in their proton affinity. In goethite two types of triply coordinated groups are found, one protonated (Fe_3OH) and one nonprotonated (Fe_3O). The proton–oxygen bond of the protonated $Fe_3OH^{1/2+}$ group is stronger than the proton–oxygen bond of the nonprotonated $Fe_3O^{1/2-}$ group. This concept can be applied to the surface structure exposed by the imaginary cut in Fig. 4 where one third of the triply coordinated surface groups has a H bond with the singly (Fe) coordinated surface group. This configuration is very stable, i.e., the proton affinity is high and the degree of protonation is hardly affected by pH. According to the structure, the two other types of triply coordinated surface groups are a hydroxyl and an oxygen, reflecting the difference in their proton affinities. The situation can be simplified if the difference in proton affinity between two types of triply coordinated groups is very large. It has been shown (16) that where there is large difference in proton affinity (large ΔpK) such types of surface species may become completely oppositely charged if present in a 1:1 ratio. For goethite this leads to $Fe_3O^{-1/2}$ species dominating the low affinity sites, and to $Fe_3OH^{+1/2}$ species dominating the high affinity sites. We consider the most inner-oriented triply coordinated surface groups as representative of this combination, i.e., the combination is zero charged over a large pH range. As a result, the charging behavior of goethite is probably determined by the remaining surface groups (shaded in Fig. 4), namely the singly coordinated FeOH(H) and a triply coordinated $Fe_3O(H)$. As mentioned above, in order to maintain reactivity, these two types of surface groups cannot have a large difference in proton affinity.

The above surface structural analysis is supported by our experience of PO_4 adsorption modeling for goethite. We have found that a complete description of PO_4 adsorption phenomena is only possible if the total site density of proton reactive groups is set to about 6 nm^{-2}, which is equivalent to two rows of reactive groups (FeOH(H) and $Fe_3O(H)$) per unit cell length of the 110 face. In our simplifying approach the proton affinity of the singly and triply coordinated surface group is set equal which means that the log *K* value equals the value of the point of zero charge (18, 55, 56). Phosphate is thought to react only with the singly coordinated surface groups (9, 19).

The 021 plane is exposed at the ends of the goethite needle. The length of the crystals will determine its relative abundance which is often less than 10%. The 021 plane is characterized by alternating rows of singly and doubly coordinated surface groups. The site density of each type of group on this 021 face is about 7.4 nm^{-2}. The chemical composition of this plane is given in Fig. 5.

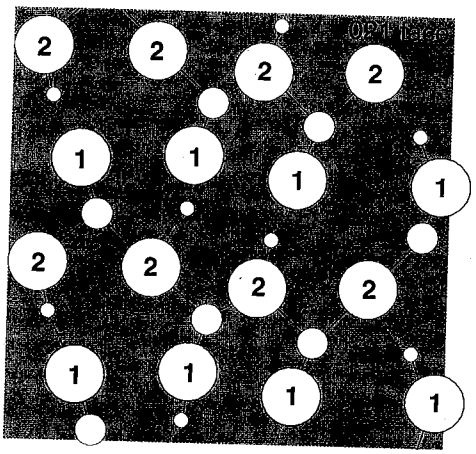

FIG. 5. A schematic representation the surface structure of the 021 face of goethite in which singly and doubly coordinated oxygens (large circles) are present in rows. The numbers refer to the coordination number with Fe^{+3} ions (small circles). The singly coordinated surface groups are raised above the doubly coordinated surface groups. Hydrogens bonds are present between the singly and doubly coordinated surface groups.

EXPERIMENTAL

Three batches of pure crystalline goethite suspensions were made by slowly neutralizing freshly prepared 0.5 *M* Fe nitrate solution with 2.5 *M* NaOH, followed by aging at pH 12 for 90–110 h in an oven (60°C) and dialysis for 2 weeks (16). All solutions were prepared with double-distilled water and contact with glassware was avoided. Each batch was characterized using transmission electron microscopy (TEM), X-ray diffraction of a random powder specimen, and thermogravimetric analysis (TGA). Also the BET surface area of the individual batches was determined by N_2 gas adsorption. This characterization indicated that the preparations contained pure nonporous goethite particles of mainly monodomainic crystals, and were therefore identical with the preparation discussed previously (16). The charging curves of the individual batches were determined using the method described elsewhere (16). These experimental data showed that goethite crystals could be reproducibly prepared with only minor differences. For the adsorption experiments, a stock suspension was made by mixing three individual goethite suspensions. The electromobility of the stock suspension was measured in the pH range 8.5–10 in 0.01 *M* $NaNO_3$ without any attempt to exclude CO_2 using a Malvers Zetasizer III.

The type of crystal planes developed on the goethite crystals of our preparation was assessed from the shape of the crystals perpendicular to the *c* axis as determined by TEM. Thin sections were made for TEM examination by embedding the goethite in a synthetic organic polymer.

The PO_4 adsorption isotherms were measured at four different pH levels (pH 4, 7, 9, and 11) in 0.01 *M* $NaNO_3$. CO_2-free NaOH solutions were made from a highly concentrated 1:1 $NaOH/H_2O$ mixture which had been centrifuged in order to remove any solid Na_2CO_3. The supernatant was pipetted into boiled double-distilled water and stored in a plastic bottle placed in a CO_2-free desiccator equipped with a CO_2 absorbing column. About 60 ml of the diluted goethite suspension in 0.01 *M* $NaNO_3$ was placed in a thermostated vessel (20 ± 0.1°C) and brought to pH 4 for 1 h with 0.01 *M* HNO_3/0.01 *M* $NaNO_3$ to remove (bi)carbonate by purging purified moist N_2-gas. Next the pH of the sample was raised with 0.01 *M* NaOH to the appropriate pH of the experiment. The sample was kept (pH-stat) at this pH for about 1 h in order to reach equilibrium before a known volume of 0.005 *M* NaH_2PO_4/0.005 *M* $NaNO_3$ was added. After equilibration at the given pH for 20 h (pH-stat) under continuous purging with N_2-gas, a sample was taken under N_2, and centrifuged at high speed without contact with air. The supernatant was filtered through a 0.025 μm filter to remove any fine particles. The P concentration was measured colorimetrically by the molybdate blue method.

Based on a proper bookkeeping of the added volumes and concentrations of the chemicals NaH_2PO_4, HNO_3, and NaOH and the experimentally measured equilibrium P concentration and pH, it is possible to calculate both the adsorption of PO_4 and the simultaneous adsorption of H^+ ions (or desorption of OH^-). The adsorption of H^+ is found from the net difference of the protons added (NaH_2PO_4, HNO_3, and NaOH) and the amount of remaining H left in solution after equilibration, according to

$$H_{ads} = H_{added} - \Delta H_{sol}$$

with

$$H_{added} = 2V_1C_{NaH_2PO_4} + V_2C_{HNO_3} - V_3C_{NaOH}$$

and

$$\Delta H_{sol} = V_t(3[H_3PO_4] + 2[H_2PO_4^-] + 1[HPO_4^{-2}] + 1[NaHPO_4^{-1}]) + \Delta V(H^+ - OH^-),$$

in which V_t is the total volume of the system after addition of phosphate solution (V_1), acid (V_2), and/or base (V_3), and $\Delta V = V_1 + V_2 + V_3$. The concentration of the solution species $[H^+]$, $[OH^-]$, $[H_3PO_4]$, $[H_2PO_4^{-1}]$, $[HPO_4^{-2}]$, and $[NaHPO_4^{-1}]$ were calculated from the experimental pH and P concentration. The intrinsic formation constants used for the calculation of the solution speciation are given in Table 1 and the activity coefficient f_k for a species k was calculated using the Davies equation (45, 58, 59),

$$\log f_k = -0.51z_k^2\left\{\frac{\sqrt{I}}{1+\sqrt{I}} - 0.2I\right\}, \qquad [17]$$

where I is the ionic strength and z_k is the valence of the species.

TABLE 1
Aqueous Speciation Reactions with Equilibrium Constants Taken from Smith and Martell (57)

Species	Reaction	Log $K°$
HPO_4^{-2}	$PO_4^{-3} + H^+ \leftrightarrows HPO_4^{-2}$	12.35
$H_2PO_4^{-1}$	$PO_4^{-3} + 2H^+ \leftrightarrows H_2PO_4^{-1}$	19.55
$H_3PO_4^0$	$PO_4^{-3} + 3H^+ \leftrightarrows H_3PO_4^0$	21.70
$NaHPO_4^{-1}$	$PO_4^{-3} + H^+ + Na^+ \leftrightarrows NaHPO_4^{-1}$	13.4
H_2O	$H^+ + OH^- \leftrightarrows H_2O$	14.0

BASIC CHARGING BEHAVIOR

Application and validation of the CD model starts with the description of the basic charging behavior of goethite.

Experimental Results

The charging behavior of *Me* (hydr)oxides is a basic property, from which the intrinsic double layer properties of the interface can be found, in particular the overall capacitance C of the Stern layer. Also the possibility of ion pair formation can be evaluated and reaction constants for ion pair formation can be assessed.

The charging behavior of the goethite used in this study is shown at three electrolyte concentrations in Fig. 6. The data points represent the weighted mean of the charging curves of the individual preparations with charge expressed per unit surface area using the weighted mean BET surface area ($A = 105 \pm 5$ m^2/g). The PZC derived from the titration curves was 9.5 ± 0.1 which corresponds with the isoelectric point (IEP) for the bulked suspension in 0.01 M $NaNO_3$ (IEP = 9.4 ± 0.1).

Modeling the Surface Charge

The surface charge for goethite can be described within the CD concept by assuming that the charging of the 110 face of goethite is related to the presence of a row of singly coordinated FeOH(H) surface groups and a row of Fe_3O(H) surface groups per unit cell length. The singly coordinated surface groups may protonate in principle by two consecutive steps (Eq. [3]). However, the very high proton affinity of the $FeO^{-3/2}$ group, predicted by the MUSIC model (15), leads to the conclusion that the dominant singly coordinated species will be $FeOH^{-1/2}$ and $FeOH_2^{+1/2}$, i.e., the charging behavior will be determined by

$$FeOH^{-1/2} + H^+ \leftrightarrows FeOH_2^{+1/2} \quad K_{1,2}. \qquad [18]$$

Only one protonation step for triply coordinated surface groups can be defined:

$$Fe_3O^{-1/2} + H^+ \leftrightarrows Fe_3OH^{+1/2} \quad K_{3,1}. \qquad [19]$$

A second protonation step is not possible because all four orbitals of the oxygen in the Fe_3OH species are already occupied.

As discussed above, the log K values of the two protonation reactions (Eqs. [18] and [19]) cannot be too different. At present the precise log K values are unknown and we therefore set them to be equal. For a surface with only one protonation reaction, such as Eq. [18] or Eq. [19], the corresponding log K value can be found directly from the PZC (18, 55). This implies a value for the protonation constants log $K_{1,2}$ and log $K_{3,1}$ of 9.5 for our goethite preparation. A distinction between the two proton reactive groups is still important because only singly coordinated groups are active in oxyanion binding such as PO_4 (9, 19).

Assuming the presence of ion pairs, the corresponding reactions can be given as

$$FeOH^{-1/2} + Na^+ \leftrightarrows FeOH^{-1/2} - Na^+ \quad K_{c1} \qquad [20]$$

and

$$FeOH_2^{+1/2} + NO_3^- \leftrightarrows FeOH_2^{+1/2} - NO_3^- \quad K_{a2}. \qquad [21]$$

For the triply coordinated groups similar reactions can be defined:

$$Fe_3O^{-1/2} + Na^+ \leftrightarrows Fe_3O^{-1/2} - Na^+ \quad K_{c2} \qquad [22]$$

and

$$Fe_3OH^{+1/2} + NO_3^- \leftrightarrows Fe_3OH^{+1/2} - NO_3^- \quad K_{a2}. \qquad [23]$$

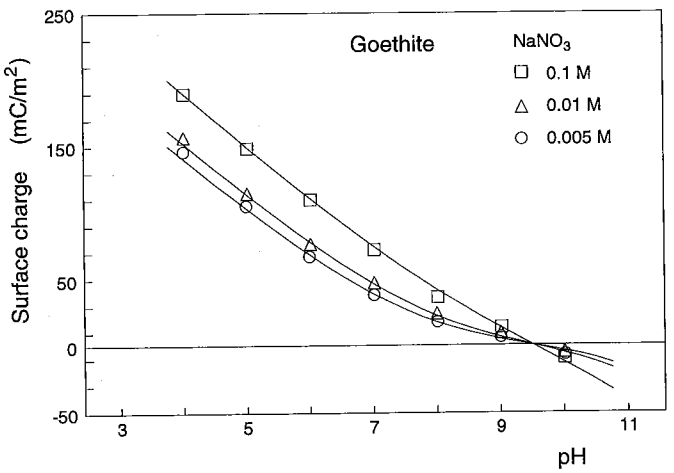

FIG. 6. The experimental charging behavior of goethite at three different concentrations of $NaNO_3$ (interpolated points). The lines correspond to calculated charging curves using $N_s = N_{s,1} + N_{s,2} = 3.45 + 2.7 = 6.15$ nm^{-2}, $C = 0.9$ F/m^2, and log $K_{1,2}$ = log $K_{3,1}$ = 9.5 and log K_c = log K_a = −1 (BS approach with ion pairs in the d-plane, see text for details and definitions).

In the CD model with the three plane (TP) approach, the ion pairs are assumed to be present in the plane at the head end of the DDL (2- or d-plane). We assume symmetrical ion pair formation, i.e., $K_{c(i)} = K_{a(i)}$.

In the calculation of the surface charge a value for the site density N_s is required. This should be related to the chemical composition of the surfaces. TEM of thin sections perpendicular to the c direction showed wedge-shaped crystals characteristic of the presence of the 110 face and its equivalents. The goethite crystals in our preparation were very elongated which implies that the 110 face was dominant. Using the measured crystal dimensions, the surface area of the faces at the head end of the crystal (021 face) was estimated to be about 5% of the total surface area. An AFM study of goethite (54) has recently shown that the contribution of the 021 face may be significant due to the presence of numerous steps on the dominant faces. The 021 face has a reactive site density for singly coordinated groups of $N_s = 7.4$ nm^{-2}, being slightly higher than the total reactive site density (singly and triply coordinated groups) of the 110 face ($N_s = 6$ nm^{-2}). For reasons of simplicity, we consider the goethite interface as a single electrostatic face (see Discussion). The charging behavior of goethite is not very sensitive to the precise value of the total site density, but the site density is critical for PO_4 modeling because the PO_4 affinity for singly coordinated surface groups is so high that site saturation may occur at low pH values. This implies that the value of N_s determines the P adsorption behavior and means that the site density of singly coordinated surface groups to be used in the modeling is somewhat greater than the value calculated for the 110 face alone ($N_s = 3$ nm^{-2}). The contribution of the 021 face, having a very high site density for singly coordinated groups, and the potential presence of defects must also be included. We have assumed site densities for the surface groups equivalent to a mixture of 10% 021 face and 90% 110 face, yielding a site density for singly ($N_{s,1}$) and triply ($N_{s,2}$) coordinated surface groups of 3.45 and 2.7 nm^{-2}, respectively.

A good description of the data can be found by assuming symmetric ion pair formation with $\log K_c = \log K_a = -1$ for both singly and triply coordinated surface groups. The charging curves, shown in Fig. 6, have been calculated with a value for the overall Stern layer capacitance, C, of 0.9 F/m^2.

CD ION ADSORPTION MODELING

PO_4 Adsorption

PO_4 adsorption on goethite is strongly related to the charging behavior of the *Me* (hydr)oxide. As shown by Hiemstra *et al.* (16), the experimental charging capacity for goethite may vary strongly depending on its method of preparation. Goethites with specific surface areas less than about 50 m^2/g are generally multidomainic, having a large number of imperfections (46). The charging behavior of these preparations is characterized by a large experimental capacitance (slope C/m^2/ΔpH) (16, 39).

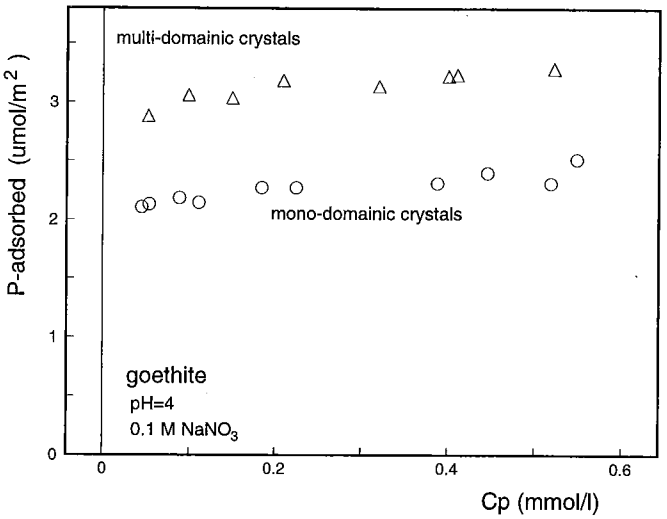

FIG. 7. The adsorption of PO_4 by a mainly monodomainic goethite with a low surface charge density (high surface area A) and a multidomainic goethite with a high surface charge (low surface area A) at pH 4 in 0.1 M $NaNO_3$ as function of the total orthophosphate concentration (C_p), illustrating the relation between surface charging and anion adsorption capacity.

Our goethite preparation, made by the slow neutralization of Fe nitrate solution, has a high specific surface area (A = 105 m^2/g), and TEM observations showed well developed monodomainic crystals. The charge density of this goethite is considerably lower than multidomainic goethite preparations. This can be illustrated by comparing the charge of this goethite with one made by the very rapid neutralization of Fe nitrate solution (A = 38 m^2/g). The experimental surface charge for these goethites at pH 4 in a 0.1 M $NaNO_3$ solution was about 190 and 300 mC/m^2, respectively.

The difference in proton reactivity may affect the adsorption behavior of PO_4. A higher positive surface charge at low pH induces a higher adsorption capacity for negative anions like PO_4, because more negative charge can be brought to the surface for a given change in electrostatic potential. Large adsorption densities are only possible if a sufficient number of sites is available. The enhanced anion adsorption for goethites with a high surface charge is shown in Fig. 7. The combination of a low surface area, a very high surface charge, and a high PO_4 adsorption capacity (measured on a surface area basis) can also be found in the literature. Sigg and Stumm (28) reported PO_4 adsorption values of more than 5 μmol/m^2 at pH 4 in a similar concentration range to that given in Fig. 7. Only carefully chosen anion adsorption data sets should be compared directly.

The adsorption of PO_4 in 0.01 M $NaNO_3$ was determined at four pH values. Great care was taken to avoid contamination with Si and $(H)CO_3$. The data set is presented in Fig. 8 together with the data set of Bowden *et al.* (26), who

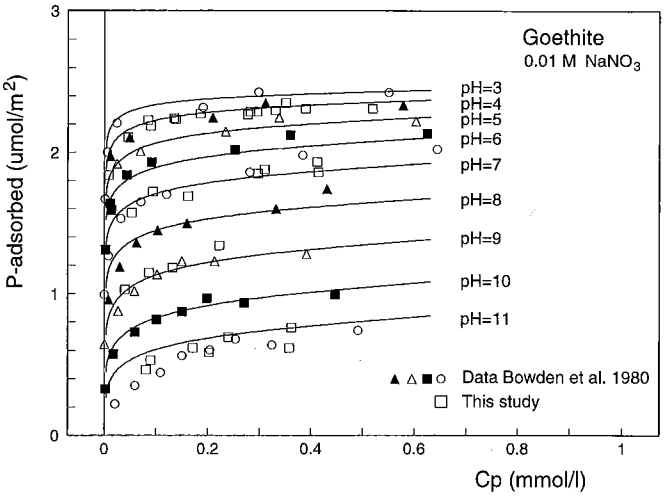

FIG. 8. The adsorption of PO_4 by monodomainic goethite used and that of Bowden *et al.* (26). The lines are calculated with the CD model and are consistent with the surface species observed by CIR-FTIR spectroscopy.

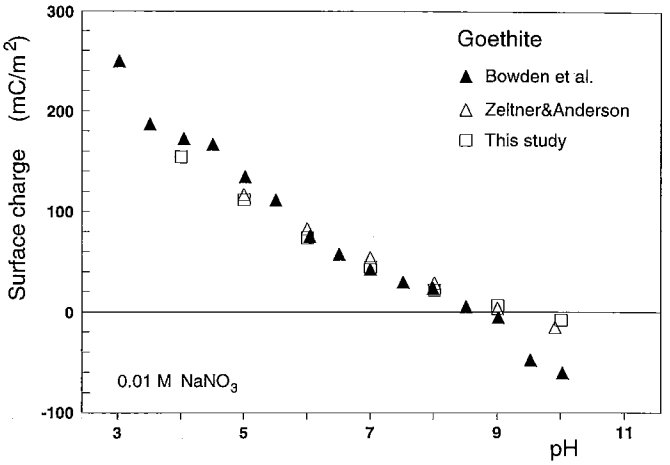

FIG. 10. The surface charge in 0.01 *M* electrolyte for the goethites used in the PO_4 adsorption analyses. Data of Bowden *et al.* (26), Zeltner and Anderson (60), and this study.

studied the PO_4 adsorption under the same conditions (pH, P concentration and electrolyte concentration). Both goethite preparations have a high surface area (A = 105 and 80 m^2/g, respectively), which makes it possible to compare the experimental results.

The PO_4 adsorption data for a goethite which was used to examine the surface PO_4 speciation (13) by CIR-FTIR spectroscopy are also considered. In this case, the PO_4 adsorption isotherms were determined over a 10-fold higher PO_4 concentration range. The surface area of this goethite was also high (A = 81 m^2/g). The isotherms are presented in Fig. 9, together with the calculated adsorption using the CD model with the same parameters as used in Fig. 8.

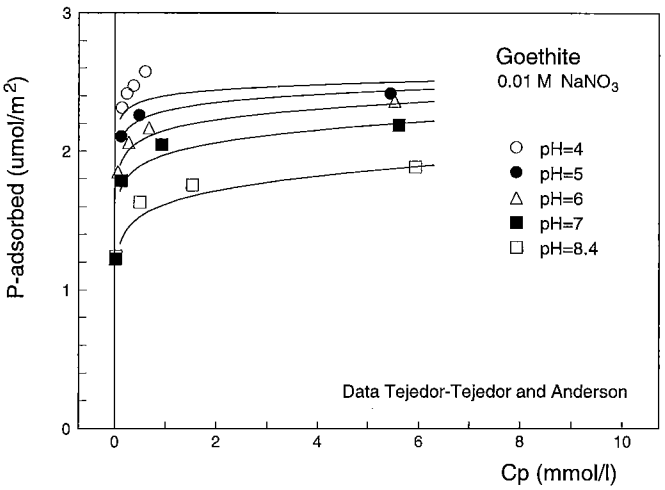

FIG. 9. The adsorption of PO_4 by the goethite of Tejedor-Tejedor and Anderson (13) (A = 81 m^2/g), over a tenfold higher phosphate concentration range compared with Fig. 8. The lines are calculated with the CD model using the same parameters as for Fig. 8.

The remarkable similarity in PO_4 adsorption behavior for the three data sets indicates that the charging of these goethites is essentially the same, which is confirmed by a comparison of the charging curves (Fig. 10) in the 0.01 *M* electrolyte. Only a distinctive difference in charging is observed for the σ_0–pH curve of Bowden *et al.* (26) above pH 9. The asymmetry of the curve could be an indication of carbonate contamination. The other two goethites have PZC values of 9.0 (60) and 9.5 ± 0.1 (this study). In the calculations we have used a mean value for the PZC of 9.2, leading to $\log K_{1,2} = \log K_{3,1} = 9.2$. The capacitance C was set to 0.9 F/m^2 as used in the calculations in Fig. 6. In all three cases a good agreement exists between the PO_4 adsorption data and the CD model results.

Surface PO_4 Speciation

The choices of species and parameters for the description of the PO_4 surface speciation are strongly constrained by the CIR-FTIR measurements. The IR data show that from pH 3.5–8 the dominant PO_4 surface species is a bidentate complex $Fe_2O_2POO(H)$ ($\geq$85%) which is protonated at low pH. The pH at which the protonation of the surface complex occurs is related to the total amount of PO_4 adsorbed. At high PO_4 loading the presence of the protonated Fe_2O_2POOH species becomes important because increased adsorption of PO_4 decreases the particle charge and may even cause charge reversal thereby enhancing protonation.

In Fig. 11 the relative abundance of both bidentate surface species is shown for three different concentrations of added PO_4. The relative presence has been derived from the computed peak areas for the different adsorption bands given by Tejedor-Tejedor and Anderson (13) assuming that all complexes had a similar extinction coefficient. They assigned the 1123 ± 4 and 1006 ± 4 cm^{-1} bands to the proton-

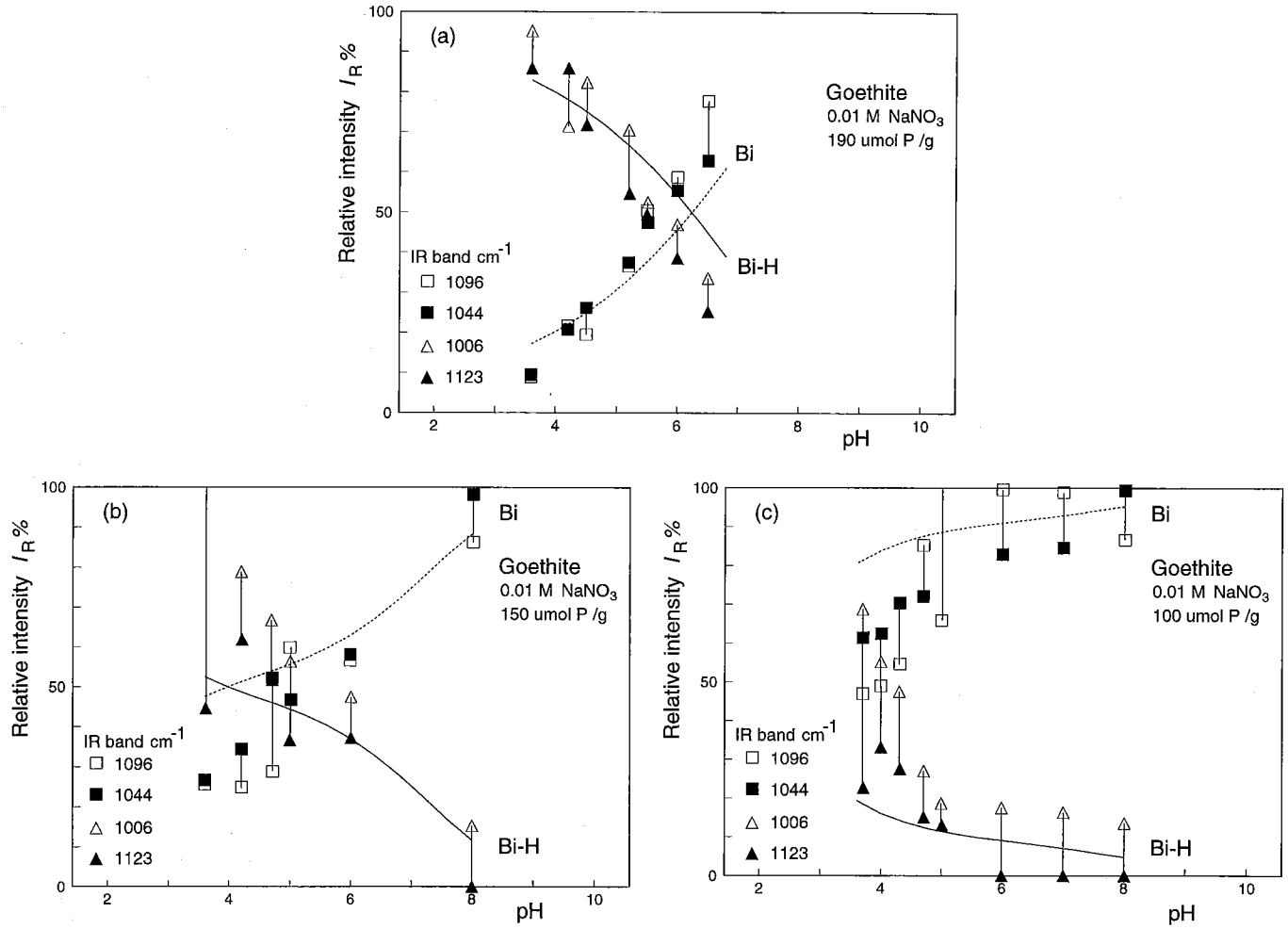

FIG. 11. The increase of the relative intensities I_R of the bidentate Fe_2O_2POOH peak (Bi–H) and corresponding decrease of the intensity of the Fe_2O_2POO peak (Bi) for three different PO_4 loadings: (a) 190 μmol/g, (b) 150 μmol/g, and (c) 100 μmol/g (A = 81 m^2/g). The data indicate that protonation increases with PO_4 loading. The lines are calculated using the CD model. Data: Tejedor-Tejedor and Anderson (13).

ated bidentate Fe_2O_2POOH species and the 1096 ± 6 and 1044 ± 6 cm^{-1} bands to the nonprotonated $Fe_2O_2PO_2$ species. We have assumed that each of the two peaks is representative for a particular phosphate surface complex and so have normalized the peak area of each species relative to the sum of the four above mentioned peaks. This yields a measure for the abundance of each species. This is plotted in Fig. 11 as the relative intensity, I_R. Note that the nonprotonated bidentate surface species at pH 4 is only 20% at the lowest loading, whereas its abundance increases to more than 80% at the same pH when the P loading is doubled.

Besides the presence of bidentate complexes, the presence of monodentate complexes in the pH range 3.5–8 has also been reported. The possibilities for a quantitative interpretation are, however, rather limited due to low sensitivity at low species concentration observed. A semi-quantitative interpretation of the intensity of the 1025 ± 2 cm^{-1} band suggests an increased abundance of monodentate species with increasing pH and, interestingly, a relative decrease in abundance of monodentate species with increased PO_4 loading (Fig. 12). This decrease arises from the presence of three highly negatively charged ligands in the 1-plane which leads to an asymmetrical charge distribution in the monodentate species. With increasing PO_4 loading, the 1-plane becomes strongly negatively charged, favoring the presence of bidentate species which introduce less charge into the 1-plane.

Detailed Modeling

The adsorption reactions of PO_4 have been given for bidentate and monodentate surface complex formation earlier (Eqs. [7], [10], and [12]). The precise value for the charge distribution factor, f, has to be adjusted. For simplicity, one could assume that f does not change for bidentate species as a result of protonation and that the monodentate complex has a value for f of half of the value found for the bidentate complex because the number of common surface ligands is

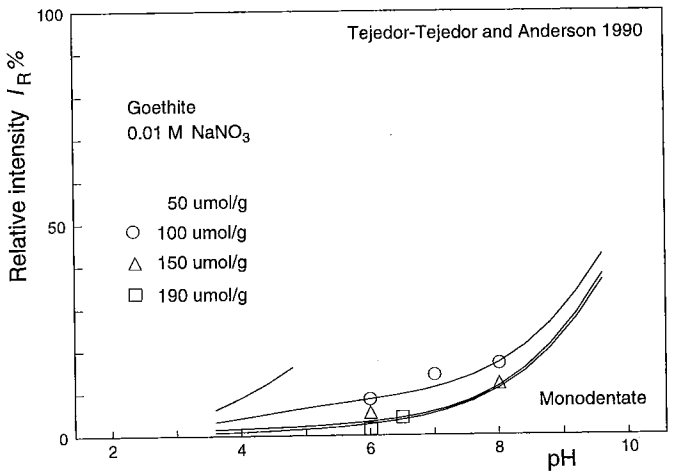

FIG. 12. The increase in the relative intensity I_R of the monodentate $FeOPO_3$ peak for three different PO_4 loadings. The data indicate a decrease in monodentate surface complexation with increasing PO_4 loading. The lines in the figure are calculated using the CD model. Data: Tejedor-Tejedor and Anderson (13).

half. However, the model only fitted the data well if we assigned a slightly larger value of f to the protonated bidentate species in comparison with the nonprotonated species. This implies that two f factors have to be adjusted. For the nonprotonated bidentate species the value of f of the central ion was found to be about $f = 0.5$, which is identical to the value that would be expected from Pauling's charge distribution concept using an equal distribution over all oxygen ligands. The monodentate complex has one bond with a surface group and the value of f is set to half the value of the bidentate complex, leading to $f = 0.25$. The value of f for the protonated bidentate complex was set higher at $f = 0.6$. This higher value is equivalent with an additional charge transfer toward the surface of half a unit charge due to protonation.

Initially we explored the possibility of describing the data assuming the presence of only two electrostatic planes representing a basic Stern approach, i.e., a 0-plane for the adsorption of H and common surface ligands and the 1- or d-plane for the adsorption of ion pairs and solution-oriented ligands. The parameters used assuming only two electrostatic planes are given as Case I in Table 2. All of the adsorption phenomena illustrated above, including the IR surface speciation (except monodentate surface species formation) and the particle charge, could be described with this approach, except for the salt dependency. The observed salt dependency of PO_4 adsorption is small, while the predicted salt dependency based on the BS approach is large. Analysis of this discrepancy indicated that the interaction between ion pairs and the adsorbed PO_4 was too high. This implies that the solution-oriented ligands should not be placed in the same electrostatic plane as the ion pairs. For this reason a separate plane was added, splitting the Stern layer region in two parts, yielding the three plane (TP) model.

The TP approach enabled all adsorption phenomena, including the salt dependency, to be described very well (Case II and III). The modeling did not require the assumption of the presence of a monodentate complex. The corresponding parameters are given as Case II in Table 2. However, the IR bands indicate the presence of the monodentate species at high pH and low PO_4 loading (Fig. 12). For a complete description, we took into account the monodentate species (Case III in Table 2). The CD model then predicts monodentate binding that is quantitatively in agreement with the observed increase in monodentate adsorption with increasing PO_4 loading. Monodentate complexes have been observed even at a very low P loading of 50 μmol/g $\approx$ 0.6 μmol/m^2 at pH 4 (13), as predicted by the CD model ($\approx$10%, Fig. 12). Detailed information about the formulation of the model in terms of the table of species, which forms the basis of speciation calculations, is given in the Appendix. The TP model requires a capacitance to be defined for both layers. They were derived from the salt dependency of specifically adsorbing ions.

Salt Dependency

In the TP approach, an important factor influencing the salt dependency is the position of the mid-plane (1-plane), i.e., the distance between the 1- and d-plane, which is reflected in the value of the capacitance C_2. The solution-oriented ligands of the adsorbed PO_4 molecule are placed in the 1-plane and the ion pairs in the 2- or d-plane. If the distance between these planes is increased (C_2 decreases), both planes with their adsorbed species will interact less, decreasing the salt dependency. Another factor is the distribution of the charge of the phosphate ion between the two adsorption planes (0, 1-plane). In the case of monodentate adsorption (high pH), a greater proportion of the negative charge is placed in the 1-plane, leading to a stronger salt dependency.

TABLE 2

Surface Parameters Used in the Modeling of the PO_4 Data Sets (13, 26, and This Study) for Three Different Options

		Value		
Parameters	Eq.	Case I	Case II	Case III
C(F/m^2)	[4]	0.9	0.9	0.9
C_2(F/m^2)	[4]	—	5	5
log K_{in1}	[7]	—	—	20.8
log K_{in2}	[10]	29.0	29.2	29.2
log K_{in3}	[12]	35.3	35.4	35.4
log K_H	[18], [19]	9.2	9.2	9.2

Note. Case I: BS approach without monodentate surface species. Case II: TP approach without monodentate surface species. Case III: TP approach with mono- and bidentate surface species.

TABLE 3
Surface Parameters (TP Approach) Used in the Description of the PO_4 Data Set of Barrow *et al.* (27), Shown in Fig. 13.

Parameter	Value
C(F/m^2)	0.9
C_2(F/m^2)	5
Log K_{in1}	19.5
log K_{in2}	27.8
log K_{in3}	33.8
log K_H	8.3

Note. The log K values differ from the values given in Table 2 (Case III) because of the different log K_H used.

There is only one extended data set on PO_4 adsorption in the literature that describes the salt dependency of the PO_4 adsorption on goethite as a function of pH and PO_4 concentration (27). The goethite of Barrow *et al.* (27), however, has a relatively low PZC (PZC = 8.3). In the PO_4 modeling we have used this PZC value to define the protonation constants log $K_{1,2}$ and log $K_{3,1}$. The value for the capacitance was set equal to that found for the other goethites. Because of the different protonation behavior, the PO_4 adsorption constants (log $K_{in1\text{-}3}$) had to be adjusted (Table 3). The charge distribution has not been changed. The modeling showed that the salt dependency could be described well if the value of the outer layer capacitance was set equal to about 4–5 F/m^2.

It is possible to interpret the capacitance value in terms of a distance, d, if the dielectric constant is known. Both are related according to

$$C = \frac{\epsilon_0 \epsilon_r}{d}, \qquad [24]$$

in which ϵ_0 and ϵ_r are the absolute and relative dielectric constants. At the interface the dielectric properties change from a high value at the solution side (ϵ_r water = 80) to a low value in the solid (ϵ_r goethite = 11). If the dielectric properties of the outer layer are equal to that of water, the above given capacitance value C_2 is equivalent to a distance of about 0.13 nm between the 1- and d-plane. If the value of the dielectric constant is reduced in the vicinity of the goethite solid, for instance to about half the value of water, the distance doubles and will be in the order of the diameter of a water molecule. From this analysis it can be concluded that the calculated distances are in reasonable agreement with the expected distances based on the molecular view of the interface presented above (Fig. 2); i.e., the separation between the 0- and d-planes is equivalent to the size of a half or a whole water molecule.

Particle Charge

An interesting aspect of the ion adsorption is the change of particle charge resulting from the adsorption. This change of particle charge is the net result of specific adsorption of cations and anions and the simultaneous adsorption or release of protons from the surface. The particle charge can be defined as the sum of the surface charge σ_0 (0-plane) and the charge of the 1-plane (σ_1). The adsorption of a cation generally leads to the release of protons and/or other competing cations, resulting in a pH decrease. In contrast, the adsorption of anions generally shows an increase of pH. This experimental behavior can be predicted when a mechanistic adsorption model is used.

The number of protons needed to keep the pH constant has been measured as function of the amount of PO_4 adsorbed and the corresponding H adsorption can be calculated (Fig. 14). The

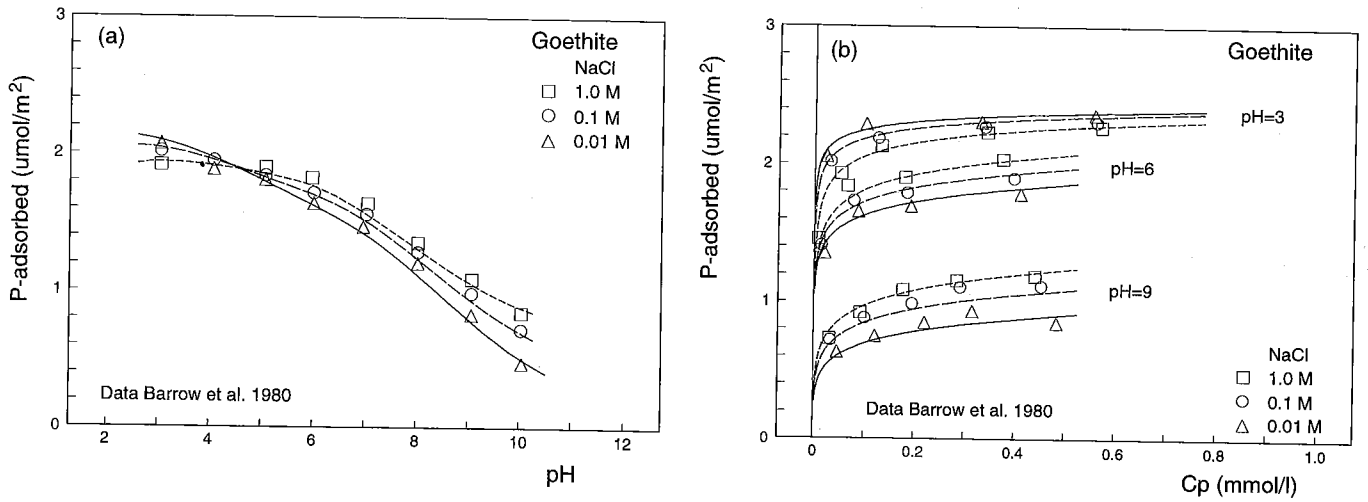

FIG. 13. (a) pH dependent adsorption of PO_4 on goethite for three concentrations of background electrolyte; (b) adsorption isotherms for phosphate as a function of pH and salt concentration. The lines were calculated using the CD model. Data: Barrow *et al.* (27).

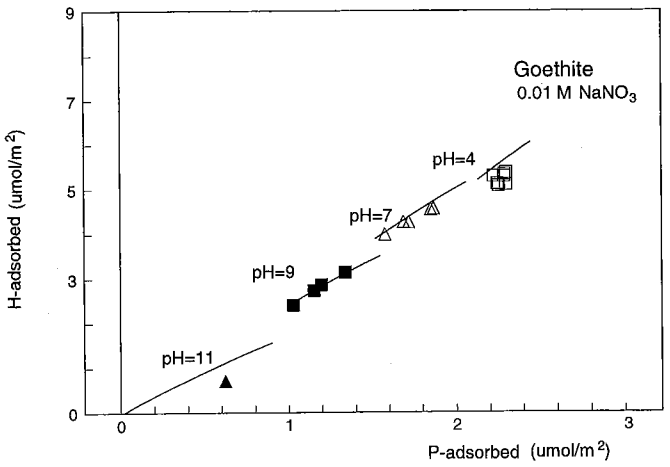

FIG. 14. The simultaneous adsorption of protons as a function of phosphate adsorption at various constant pH values (this study). The lines are based on the CD model.

predicted H adsorption upon PO_4 adsorption using the CD model closely matches the observed stoichiometry, namely 2.5 to 1.

Another type of experimental data which is related to particle charge is the electromobility. This mobility may be interpreted, within limits, in terms of a potential at the imaginary plane of shear (2). This potential is called the ζ (zeta) potential. The measurement of the mobility as a function of pH leads to a pH at which the particle as a whole is apparently uncharged. This pH is called the isoelectric point (IEP). Tejedor-Tejedor and Anderson (13) have measured the electromobility of goethite as function of pH and P loading for a system in which the adsorption and IR data were also collected (Figs. 9 and 11). This mobility has been transformed into a zeta potential (Fig. 15). It is possible to model the zeta potential if the position of the plane of shear is known. In earlier model approaches (37), it was assumed that this position is identical with the head end of the diffuse double layer (d-plane). In the CD model hydrated ion pairs are bound in this plane, which supports the idea that the shear plane is somewhat further away from the surface. This is also sometimes assumed in the literature (5, 61).

Modeling indicates that in a 0.01 M monovalent electrolyte the shear plane should be set about 0.5–1 nm from the 2- or d-plane, a distance equivalent to the thickness of 2 or 3 water molecules. Modeling two zeta potential data sets (35, 38) of *Me* (hydr)oxides indicates that the distance d between the shear plane and the head end of the DDL can be related empirically to the electrolyte concentration c, according to $d = k\, c^{1/n}$. As indicated above, a quantitative interpretation of the zeta potential is accompanied by some uncertainty. The prediction of the IEP is more straightforward (6). In that case it is assumed that the charge within the plane of shear is zero. This occurs if the potential at the head end of the DDL is zero. Calculations with the CD model show that the IEP can be predicted fairly well (Fig. 15).

DISCUSSION

We have shown that a wide range of adsorption phenomena can be described well with the CD model. It should be kept in mind that the various phenomena were not measured for a single goethite preparation, which may reduce the possibility of finding accurately a single set of parameters for describing all the adsorption phenomena. Individual phenomena could have been described better if they had been optimized separately. With the CD model it is relatively easy to describe the pH-dependent adsorption isotherms. Problems arise when the other observations must also be described with the same set of parameters. One of the major difficulties in the modeling was the attempt to describe the observed surface speciation (IR) in combination with the shift of the IEP with increasing PO_4 loading. A rather high value for the protonation constant was necessary to give a good description of the IR data over the whole range of PO_4 loading. However, this can give an excessively high positive charge for the particle at low pH resulting in a too small shift of the IEP upon PO_4 adsorption. This behavior may be related to the presence of surface site heterogeneity.

It has been shown recently (62) using extended X-ray absorption fine structure (EXAFS) analysis that oxyanions like SeO_3 and AsO_4 may form two types of bidentate inner sphere complexes. It is likely that this will also be the case for PO_4. The type of complexes formed are related to the exact location of the adsorbed species on a crystal surface. Distances measured with EXAFS indicate two distinct locations for bidentate adsorption on goethite. The difference is based on a difference in the number of *Me*

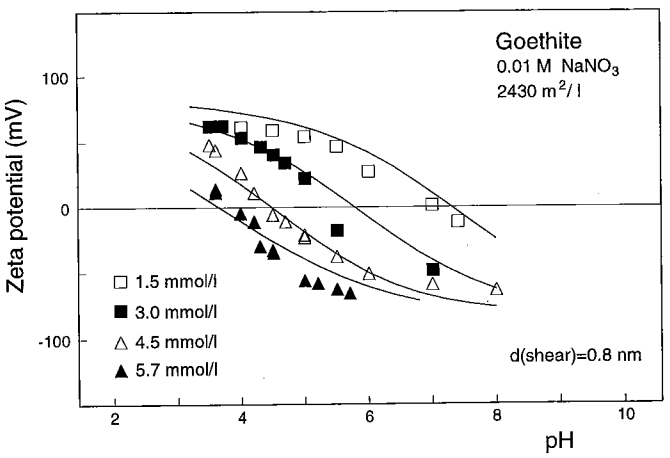

FIG. 15. The zeta potential at the plane of shear, based on the measured electromobility of a goethite suspension with various initial concentrations of PO_4 as function of pH in 0.01 M electrolyte (markers). The lines indicate the zeta potential calculated with the CD model assuming that the position of the plane of shear in solution is 0.8 nm from the head end of the DDL. Model parameters are given in Table 2 (Case III). Data: Tejedor-Tejedor and Anderson (13).

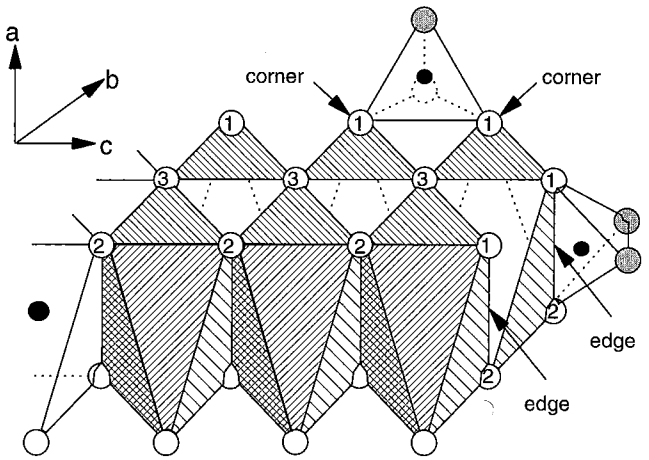

FIG. 16. A schematic representation of two rows of FeO_6 octahedra present in the goethite crystal. The numbers 1, 2, or 3 on the oxygens refer to the number of coordinating Fe^{+3} ions. Two principle types of bidentate inner sphere complex are found: bonding to the edge of one octahedron (mononuclear bidentate, ^{2}E) or to two corners of two octahedrons (bidentate binuclear, ^{2}C).

ions in the solid (n_{Me}) binding *both* ligands of the bidentate surface complex; i.e., a mononuclear (n_{Me} = 1) and binuclear bidentate complex (n_{Me} = 2) can be distinguished (Fig. 16).

The binuclear bidentate complex which is bound to two surface groups connecting the corners of two octahedrons is well known; i.e., it is called a double corner linkage (^{2}C). On goethite, this binuclear bidentate complex is dominant and can be found on the 110 face.

The two surface groups of the mononuclear bidentate complex are part of one Fe octahedron (Fig. 16). The oxyanion is therefore bound in a so-called edge linkage (^{2}E). Such edge linkages are possible for goethite on crystal faces cutting the *c* axis, such as the 021 face. On the basis of IR studies (9), it has been assumed that oxyanions are reactive with only singly coordinated surface groups. This idea was supported by the finding that PO_4 adsorption is strongly reduced if crystal planes with doubly coordinated groups are dominant (17, 22). However one of the surface groups which binds PO_4 in a mononuclear complex is not a singly coordinated FeOH surface group but a doubly coordinated Fe_2OH group. Note that, although calling the PO_4 surface complex mononuclear (only one common Fe ion with the oxygens), the total number of Fe ions involved is two.

Similar types of mono- and binuclear complexes have been established for adsorbed Cd by Spadini *et al.* (20), who found that the edge linkages can be identified as a high affinity site. If the edge bound bidentate complexes are relatively important for oxyanion binding at low loadings, the surface configuration can be characterized as being a high affinity complex. One may speculate about the reason for a high affinity character. A charge distribution factor of $f = 0.5$ in the $Fe_2O_2^{\frac{1}{2}}PO_2^{\frac{1}{2}}$ and $Fe_1O_2^{\frac{1}{2}}PO_2^{\frac{1}{2}}$ bidentate complexes leads to a value of $p = -0.5$ and $p = 0$, respectively; i.e., in the case of an edge linkage, both surface ligands in combination can be neutralized and the charge is equally distributed over inner and outer ligands $f = 0.5$. Another reason could be the difference in the angle of the orbitals in the Fe–O–P linkage, being roughly on the order of 90° and 130°, respectively.

We may apply this knowledge to the problem of matching the PO_4 IR data over the whole range of PO_4 loading and explain it on the basis of the presence of high affinity sites. The high affinity edge (^{2}E) linkages are found on the 021 face, estimated to be for goethite roughly 10% (22). At high PO_4 loading the majority of ^{2}C as well as ^{2}E sites is occupied with PO_4, so the PO_4 data are dominated by the dominant site with ^{2}C linkages (110 face). However, at a low loading the high affinity sites (^{2}E linkages) will contribute relatively more to the overall behavior than the low affinity sites, up to about 25% of the PO_4 sites at a loading of 100 μmol/g in Fig. 11c. A relatively high occupation at the 021 face will lead to a relatively greater presence of protonated bidentate surface complexes at this plane, because protonation is loading dependent (Fig. 11). Under these conditions, the contribution to the high affinity sites in the IR spectra may then be mainly in the form of the protonated Fe_1O_2POOH species, while the 110 face is still dominated by the nonprotonated $Fe_2O_2PO_2$ species. This implies that the protonated form will be underestimated at low PO_4 loading if these sites are neglected. One can model this by distinguishing two separate electrostatic surfaces, a major surface for the low affinity sites and a minor surface for the high affinity sites.

From the above analysis, one may conclude that the interpretation of the IR surface speciation at high loading is most reliable. Focusing on these data, we can model all of the other data with slightly different log K_{in2} (=29.3) and log K_{in3} (=35.3) values. The proton affinity constant of the bidentate surface complex log K_{Hp} (log K_{in3} − log K_{in2} = 6) found for our goethite in this case is equal to the log K_{Hp} (=6) found for the goethite (Table 3) with the lower PZC (Fig. 13).

A question arises as to whether the monodentate phosphate surface complex may become protonated. We have calculated the monodentate surface speciation assuming that the protonation constant log K_{Hp} found for bidentate complexes is also valid for the first protonation step for monodentate complexes. Using this value for monodentate complexes and assuming an equivalent shift of charge upon protonation (f = 0.35) indicates that at pH 4 very little protonation is likely to be observed.

It should be noted that our log K_{Hp} is considerably larger that the value that follows from the interpretation of Tejedor-Tejedor and Anderson (13). In our case, the protonation reaction involves a shift of charge from the 1-plane

to the surface, which has a higher potential, whereas Tejedor-Tejedor and Anderson attributed the net charge of the proton fully to the 1-plane. In our approach, more energy is needed to overcome the positive potential barrier, yielding a higher log K_{Hp}.

CONCLUSIONS

The charge distribution (CD) model for cation and anion adsorption can be summarized as follows:

—On the scale of the compact part of the interface, adsorbed ions should not be treated as point charges.

—Inner sphere surface complexes of cations as well as oxyanions have a spatial distribution of charge which can be attributed to two different electrostatic planes.

—The charge in the electrostatic planes results from the charge of the ligands present and of the central cation in the adsorption complex, as well as any charge which may be derived from the *Me* ions in the solid.

—The CD model is a consistent extension of the MUSIC approach for deriving the charge of surface species.

—The charge distribution of the central ion in the surface complex can be estimated from the bond valence rule.

—Inner sphere complexes of cations are generally hydroxo complexes and of oxyanions are oxo complexes; i.e., the common ligand is a hydroxyl or oxygen, respectively.

—The mean electrostatic position of outer sphere ion pairs does not coincide with the solution-oriented ligands of inner sphere complexes. This leads to a three plane approach. The outer layer capacitance C_2 is relatively high (C_2 = 4–5 F/m^2), which is equivalent to the separation of the two adsorption planes by about a half to one water molecule.

—The surface activity of adsorbed binuclear bidentate complexes should be defined in terms of coverage (θ) rather than as a concentration (mol/liter, mol/m^2).

—The CD model enables the simultaneous description of the concentration, pH, and salt dependency of adsorption and the related charge phenomena: basic proton charging, proton exchange ratio, shift of IEP and zeta potentials, in combination with the surface speciation determined by spectroscopy (*in situ* CIR-FTIR) within the constraint of an intrinsic chemical surface composition.

—Both triply and singly coordinated surface groups contribute to the charging behavior of the goethite surface, whereas only the singly coordinated surface groups are active in binding PO_4. However, both types of groups affect phosphate adsorption via electrostatic interactions.

—Triply coordinated surface oxygen groups at the goethite interface exhibit a considerable variation in proton affinity which can be related to structural differences.

—High affinity sites present on a separate electrostatic face may contribute significantly to the presence of protonated surface complexes at low phosphate loading.

—The relative decrease in monodentate oxyanion surface complexation with increasing loading and decreasing pH can be understood on the basis of electrostatics and an asymmetric distribution of charge in the interface.

—Calculations involving broken charges in surface components can be made with only a minor change in standard algorithms for speciation calculations.

APPENDIX

The formulation of the chemical equilibrium problem in terms of an ion speciation table is given in Table A for adsorption reactions. The ion speciation table relates species and components in reaction quotients and mass balances. The various components are given in the columns. In the CD model, 3 electrostatic components ($e^{-F\psi_i/RT}$) are defined for, respectively, the 0-, 1-, and 2- (or d-) plane. The chemical system of our example is built with two surface components (FeOH and Fe_3O) and four solution components (H, PO_4, Na, and NO_3). For the Na and NO_3 components a known solution concentration is assumed, reducing the number of unknown solution components to H and PO_4. The surface and the solution species concentrations are all expressed in mol/liter.

The species concentrations can be calculated by formulating the appropriate expressions with the help of the coefficients from the ion speciation table. Reading across the table, the general expression for the species concentration S (mol/liter) is

$$[S] = \Pi\,[C_k]^{n_k}\,10^{\log K}, \qquad [A\text{-}1]$$

in which the term $\Pi\,[C_k]$ is the product of component concentrations, including electrostatic components, $e^{-F\psi_k/RT}$, surface components (FeOH and Fe_3O), and solution components. The coefficients n_k are found in the rows. The log K in Eq. [A-1] is the expression given in the last column of Table A. The expression for log K can be an intrinsic equilibrium constant log K_{in} or the intrinsic equilibrium constant which includes concentration terms of the known components such as log[Na^+] or log[NO_3^-] in our example.

Two additional comments should be made about the table. The surface species in the table have to be expressed in mol/liter which is not the same as the definitions given in the text, where relative surface concentrations or mole fractions (θ) have been used. In the case of monodentate adsorption, the value of the log K is not affected by the use of mol/liter instead of mole fractions. However, for bidentate surface species the value of the log $K_{in}(\theta)$ should be rewritten as an apparent log K value, which can be used in the scheme. This leads to the derivation of a conversion factor, which converts the intrinsic adsorption constant K_{in} to an apparent constant, K_t, which can be used in the table,

TABLE A

An Example of the Table of Species for the CD–MUSIC Calculations for PO_4 Adsorption by Goethite

Components species (mol/liter)	$e^{-F\psi_0/RT}$	$e^{-F\psi_1/RT}$	$e^{-F\psi_2/RT}$	FeOH	Fe_3O	H	PO_4	log K
Na^+(aq)								0 + log[Na]
NO_3^-(aq)								0 + log[NO_3]
H^+(aq)						1		0
OH^-(aq)						−1		log K_w
PO_4^{-3}(aq)							1	0
HPO_4^{-2}(aq)						1	1	log K_{p1}
$H_2PO_4^{-1}$(aq)						2	1	log K_{p2}
$H_3PO_4^0$(aq)						3	1	log K_{p3}
$NaHPO_4^{-1}$(aq)						1	1	log K_{p4} + log[Na]
$FeOH^{-1/2}$				1				0
$FeOH_2^{+1/2}$	1			1		1		log K_{H1} = log $K_{1,2}$
$FeOH^{-1/2}$–Na^+			1	1				log K_c + log [Na]
$FeOH_2^{+1/2}$–NO_3^-	1		−1	1		1		log K_a + log K_{H1} + log[NO_3]
$FeO^pPO_3^q$	$-1 + 5f_1$	$5(1 - f_1) - 6$		1		1	1	log K_{in1}
$Fe_2O_2^pPO_2^q$	$-2 + 5f_2$	$5(1 - f_2) - 4$		2		2	1	log K_{in2} − log($\rho AN_{s,1}$)
$Fe_2O_2^pPOOH^q$	$-2 + 5f_3$	$5(1 - f_3) - 2 - 1$		2		3	1	log K_{in3} − log($\rho AN_{s,1}$)
$Fe_3O^{-1/2}$					1			0
$Fe_3OH^{+1/2}$	1				1	1		log K_{H2} = log $K_{3,1}$
$Fe_3O^{-1/2}$–Na^+			1		1			log K_c + log[Na]
$Fe_3OH^{+1/2}$–NO_3^-	1		−1		1	1		log K_a + log K_{H2} + log[NO_3]
Sum	$\frac{\rho A}{F}(\sigma_0 - \sum z_j F N_{s,j})$	$\frac{\rho A}{F}\sigma_1$	$\frac{\rho A}{F}\sigma_2$	$\rho AN_{s,1}$	$\rho AN_{s,2}$	H(t) − OH(t)	PO_4(t)	

Note. All log K values are based on intrinsic constants, adjusted for activity corrections in the case of $I \neq 0$.

$$K_{in} = \frac{\theta_{ads}}{\theta_{ref}^2 \Pi C_{k,sol}^{n_k}} = \frac{\frac{S_{ads}}{\rho AN_{s,j}}}{\left(\frac{S_{ref}}{\rho AN_{s,j}}\right)^2 \Pi C_{k,sol}^{n_k}}$$

$$= \rho AN_{s,j}\left\{\frac{S_{ads}}{S_{ref}^2 \Pi C_{k,sol}^{n_k}}\right\} = \rho AN_{s,j} K_t, \qquad [A\text{-}2]$$

in which S_{ads} is the species concentration of the adsorbed complex (mol/liter), S_{ref} (mol/liter) is the species concentration of the reference surface component (here the surface group FeOH), ρ is the solid–solution ratio (kg/liter), A is the specific surface area (m^2/kg), and $N_{s,j}$ is the site density (mol/m^2) of surface group j. In Eq. [A-2], $C_{k,sol}$ represents the various solution component concentrations. Based on Eq. [A-2], the log K_t for Table A equals log K_t = log $K_{in}(\theta)$ − log($\rho AN_{s,j}$) in the case of bidentate surface complexation. In the table of species, calculations are based on concentrations, whereas equilibria are defined in terms of activities. The necessary activity corrections can be made by introducing the activity coefficients in the log K value used in the calculations.

The table with coefficients can also be used to formulate the mass balances necessary for solving the chemical equilibrium problem. The mass balances related to the first three columns need some comments.

The mass balance formulated with coefficients from the first column expresses the change of charge (in mole unit charge = mol p^+) of the surface plane relative to the reference components chosen (FeOH and Fe_3O), expressed in mol/liter. The mass balance expresses the difference in surface charge starting from a surface with only the two surface components (FeOH and Fe_3O groups). The mass balance based on species concentrations (Σ_1) is therefore equal to

$$\Sigma_1 = \frac{\rho A}{F}(\sigma_0 - \sum z_j F N_{s,j}), \qquad [A\text{-}3a]$$

in which σ_0 is the surface charge (C/m^2) and $\Sigma\ z_j F N_{s,j}$ is the charge of the surface when only the surface components j are present (z_j of both reference components $FeOH^{-1/2}$ and $Fe_3O^{-1/2}$ equals −0.5). The charge in C/m^2 is converted to mol p^+/m^2 using $1/F$ (F = 96485 C/mol p^+) and is recalculated to mol/liter with the help of ρ (kg/liter) and A (m^2/kg).

The expression [A-3a] is different from the expression

used in the classical scheme due to the presence of the term $\Sigma\ z_j FN_{s,j}$. This term is not necessary if the charge of the reference surface component is zero, as is usually the case in calculations based on the classical 2pK approach in which SOH^0 is used as the reference component. As shown in Table A and expression [A-3a], the standard computer code has only to be extended by the term $\Sigma\ z_j FN_{s,j}$ in order to do all CD model calculations!

The value of the right-hand side of Eq. [A-3a] can be found with help of electrostatics using the potential of the 0- and 1-plane according to

$$\sigma_0 = C_1(\psi_0 - \psi_1), \qquad [A\text{-}3b]$$

in which C_1 is the capacitance of the first layer between the 0- and 1-plane.

For column 2 a similar approach is used. Here the mass balance based on surface speciation (Σ_2) is equal to

$$\Sigma_2 = \frac{\rho A}{F}\sigma_1, \qquad [A\text{-}4a]$$

in which σ_1 is the charge of the 1-plane (C/m^2) based on electrostatic calculations, according to

$$\sigma_1 + \sigma_0 = C_2(\psi_1 - \psi_2), \qquad [A\text{-}4b]$$

in which C_2 is the capacitance of the second layer between the 1- and 2- (or d-) plane.

For column 3 only a minor difference in approach is used. Here the mass balance based on surface speciation (Σ_3) is equal to

$$\Sigma_3 = \frac{\rho A}{F}\sigma_2, \qquad [A\text{-}5]$$

where σ_2 is the charge of the 2- (or d-) plane (C/m^2). The charge in the 2- (or d-) plane can also be calculated from electrostatics. It should then be realized that the charge at the interface is present in four different locations. Charge is present at the surface in the 0-plane (σ_0), in the 1-plane (σ_1), the 2- (or d-) plane (σ_2) and also in the DDL (σ_{ddl}). As a result of overall electroneutrality one may write

$$\sigma_0 + \sigma_1 + \sigma_2 + \sigma_{ddl} = 0. \qquad [A\text{-}6]$$

The surface charge (σ_0) and the charge in the 1-plane (σ_1) can be found for a given set of potentials (ψ_0, ψ_1, ψ_2) using Eqs. [A-3b] and [A-4b]. The charge in the DDL (σ_{ddl}) can be calculated, using $\psi_d = \psi_2$, according to

$$\sigma_{ddl} = \pm\frac{1}{2}\sqrt{8000\epsilon_0\epsilon_r RT}\sqrt{\sum_i C_i\{e^{-z_i F\psi_d/RT} - 1\}}, \qquad [A\text{-}7]$$

in which ϵ_r and ϵ_0 are the relative and absolute dielectric constants. Combination of Eqs. [A-3b], [A-4b], [A-6], and [A-7] finally yields the charge in the 2-plane.

The calculation procedure starts with calculation of the speciation using estimates for the component concentrations. The mass balances, based on the calculated speciation, are compared with the expressions in the last row of the ion speciation table. If the difference is greater than the expected small value, i.e., an incorrect estimation of the component concentrations, an improvement of the estimates is calculated. The calculation procedure is repeated until a sufficiently accurate numerical solution is found, applying the commonly used Newton–Raphson procedure.

ACKNOWLEDGMENTS

Mr. Th.A. Vens is gratefully acknowledged for his efforts in carefully carrying out the experimental work. Thanks are also due to Mr. A. J. Korteweg and Mr. A. J. VanderLinde (Dept. of Physical and Colloid Chemistry) for the BET analysis and the assistance in using the Zetasizer and due to Mr. J. D. J. VanDoesburg (Dept. of Soil Science and Geology) for the TGA and X-Ray diffraction analysis. Mr. H. Wijna, Mrs. E. Bou, and Mr. F. Thiel are gratefully acknowledged for their contribution in the characterization of the goethite using TEM.

The authors also express their gratitude to Professor U. Schwertmann and Dr. P. G. Weidler for their valuable contribution in the discussion about the crystal surfaces.

Part of this work was funded by a grant of the European Community, STEP CT90-0031.

REFERENCES

1. Hingston, F. J., *in* "Adsorption of inorganics at Solid-Liquid interfaces" (M. A. Anderson and A. J. Rubin, Eds.), Chap. 2. Ann Arbor Science Pub., Ann Arbor, Michigan, 1981.
2. James, R. O., and Parks, G. A., *in* "Surfaces and Colloid Science" (E. Matijevic, Ed.), Vol. 12 Chap. 2. Plenum, New York, 1982.
3. Sposito, G., "The Surface Chemistry of Soils." Oxford Univ.Press, New York, 1984.
4. Barrow, N. J., "Reactions with Variable Charge Soils." Nijhoff, Dordrecht, The Netherlands, 1987.
5. Dzombak, D. A., and Morel, F. M. M., "Surface Complexation Modeling: Hydrous Ferric Oxide." Wiley, New York, 1990.
6. Davis, J. A., and Kent, D. B., *in* "Mineral–Water Interface Geochemistry: Reviews in Mineralogy" (M. F. Hochella and A. F. White, Eds.), Vol. 23, p. 177. Miner. Soc. Am., Washington, DC, 1990.
7. Goldberg, S., *in* "Advances in Agronomy" (J. L. Sparks, Ed.), Vol. 47, p. 233. Academic Press, New York, 1992.
8. Stumm, W. "Chemistry of the Solid-water Interface." Wiley, New York, 1992.
9. Russell, J. D., Parfitt, L. R., Fraser, A. R., and Farmer, V. C., *Nature* **248,** 220 (1974).
10. Parfitt, R. L., Atkinson, R. J., and Smart, R. S. C., *Soil Sci. Soc. Am. Proc.* **39,** 837 (1975).
11. Parfitt, R. L., and Atkinson, R. J., *Nature* **264,** 740 (1976).

12. Parfitt, R. L., *Soil Sci. Soc. Am. Proc.* **43,** 623 (1979).
13. Tejedor-Tejedor, M. I., and Anderson, M. A., *Langmuir* **6,** 602 (1990).
14. Van Riemsdijk, W. H., and VanderZee, S. E. A. T. M., *in* "Interactions in the Soil Colloid–Soil Solution Interface" (G. H. Bolt, M. F. DeBoodt, M. H. B. Hayes, and M. B. McBride, Eds.), NATO ASI Series (E), Vol. 190, Chap. 8. Kluwer Academic, Dordrecht, 1991.
15. Hiemstra, T., Van Riemsdijk, W. H., and Bolt, G. H., *J. Colloid Interface Sci.* **133,** 91 (1989).
16. Hiemstra, T., De Wit, J. C. M., and Van Riemsdijk, W. H., *J. Colloid Interface Sci.* **133,** 105 (1989).
17. Van Riemsdijk, W. H., and Lyklema, J., *Colloids Surf.* **1,** 33 (1980).
18. Hiemstra, T., Van Riemsdijk, W. H., and Bruggenwert, M. G. M., *Neth. J. Agric. Sci.* **35,** 281 (1987).
19. Torrent, J., Barron, V., and Schwertmann, U., *Soil Sci. Soc. Am. J.* **54,** 1007 (1990).
20. Spadini, L., Manceau, A., Schindler, P. W., and Charlet, L., *J. Colloid Interface Sci.* **168,** 73 (1994).
21. Manceau, A., and Charlet, L., *J. Colloid Interface Sci.* **168,** 87 (1994).
22. Colombo, C., Barron, V., and Torrent, J., *Geochim. Cosmochim. Acta* **58,** 1261 (1994).
23. Pauling, L., *J. Am. Chem. Soc.* **51,** 1010 (1929).
24. Hingston, F. J., Posner, A. M., and Quirk, P. J., *Discuss. Farad. Soc.* **52,** 334 (1971).
25. Hingston, F. J., Posner, A. M., and Quirk, P. J., *J. Soil Sci.* **23,** 177 (1972).
26. Bowden, J. W., Nagarajah, S., Barrow, N. J., Posner, A. M., and Quirk, P. J., *Aust. J. Soil. Res.* **18,** 49–60 (1980).
27. Barrow, N. J., Bowden, J. W., Posner, A. M., and Quirk, P. J., *Aust. J. Soil. Res.* **18,** 395 (1980).
28. Sigg, L. and Stumm, W., *Colloid Surf.* **2,** 101 (1981).
29. Bolt, G. H., *in* "Soil Chemistry B Physiochemical Models" (G. H. Bolt, Ed.), 2nd ed., Chap. I. Elsevier, Amsterdam, 1982.
30. Sposito, G., "The Chemistry of Soils." Oxford Univ. Press, New York, 1989.
31. Stern, O., *Z. Electrochem.* **30,** 508 (1924).
32. Westall, J. and Hohl, H., *Adv. Colloid Interface Sci.* **12,** 265 (1980).
33. Yates, D. E., Levine, S., and Healy, T. W., *Chem. Soc. Faraday Trans. I* **70,** 1807–1818 (1974).
34. Sprycha, R., *J. Colloid Interface Sci.* **102,** 173 (1984).
35. Sprycha, R., *J. Colloid Interface Sci.* **127,** 12 (1989).
36. Yates, D. E., "The Structure of the Oxide/Aqueous Electrolyte Interface." Ph.D. Thesis, University of Melbourne, Melbourne, 1975.
37. Davis, J. A., and Leckie, J. O., *J. Colloid Interface Sci.* **67,** 90 (1978).
38. Davis, J. A., James, R. O., and Leckie, J. O., *J. Colloid Interface Sci.* **63,** 480 (1978).
39. Hiemstra, T., and Van Riemsdijk, W. H., *Colloids Surf.* **59,** 7 (1991).
40. Westall, J. C., *in* "Aquatic Surface Chemistry" (W. Stumm, Ed.), Chap. 1. Wiley, New York, 1987.
41. Hohl, H., and Stumm, W., *J. Colloid Interface Sci.* **55,** 281 (1976).
42. Schindler, P. W., and Stumm, W., *in* "Aquatic Surface Chemistry" (W. Stumm, Ed.), Chap. 4. Wiley, New York, 1987.
43. Bolt, G. H., and Van Riemsdijk, W. H., *in* "Interactions in the Soil Colloid–Soil Solution Interface" (G. H. Bolt, M. F. DeBoodt, M. H. B. Hayes, and M. B. McBride, Eds.), NATO ASI Series (E), Vol. 190, Chap. 2. Kluwer Academic, Dordrecht, 1991.
44. Davis, J. A., and Leckie, J. O., *J. Colloid Interface Sci.* **74,** 32 (1980).
45. Davies, C. W., *J. Chem. Soc.* 2421 (1930).
46. Cornell, R. M., Posner, A. M., and Quirk, P. J., *J. Inorg. Nucl. Chem.* **36,** 1937 (1974).
47. Schwertmann, U., and Cornell, R. M., "Iron Oxides in the Laboratory. Preparation and Characterization" Chap. 5. VCH, Weinheim, Germany, 1991.
48. Smith, K. L., and Eggleton, R. A., *Clays Clay Miner.* **31,** 392 (1983).
49. Schwertmann, U., *Clay Miner.* **19,** 9 (1984).
50. Mann, S., Cornell, R. M., and Schwertmann, U., *Clay Miner.* **20,** 255 (1985).
51. VanderWoude, J. H. A., DeBruyn, P. J., and Pieters, J., *Colloids Surf.* **9,** 173 (1984).
52. VanderWoude, J. H. A., and DeBruyn, P. J., *Colloids Surf.* **11,** (1984).
53. Amouric, M., Baronnet, A., Nahon, D., and Didier, P., *Clays Clay Miner.* **34,** 42 (1986).
54. Weidler, P. G., Schwinn, T., and Gaub, H. E., submitted for publication.
55. Van Riemsdijk, W. H., Bolt, G. H., Koopal, K. L., and Blaakmeer, J., *J. Colloid Interface Sci.* **109,** 219 (1986).
56. Bolt, G. H., and Van Riemsdijk, W. H., *in* "Soil Chemistry B Physiochemical Models" (G. H. Bolt, Ed.), 2nd ed., Chap. XIII. Elsevier, Amsterdam, 1982.
57. Smith, R. M., and Martell, A. E., "Critical Stability Constants" Vol. 4. Plenum, New York, 1981.
58. Davies, C. W., "Ion Association." Butterworths, London, 1962.
59. Morel, F. F. M., *in* "The Principles of Aquatic Chemistry." Wiley, New York, 1987.
60. Zeltner, W. A., and Anderson, M. A., *Langmuir* **4,** 469 (1988).
61. Healy, T. W., and White, L. R., *Adv. Colloid Interface Sci.* **9,** 303 (1978).
62. Manceau, A., *Geochim. Cosmochim. Acta* **59,** 3647 (1995).